Sādhanā Vol. 28, Parts 1 & 2, February/April 2003, pp. 209–246. © Printed in India

Mechanical behaviour of aluminium–lithium alloys

N ESWARA PRASAD[1], A A GOKHALE[1] and P RAMA RAO[2,*]

[1]Defence Metallurgical Research Laboratory, P.O. Kanchanbagh, Hyderabad 500 058, India
[2]Jawaharlal Nehru Centre for Advanced Scientific Research, Jakkur, Bangalore 560 064, India
[*]Present address: International Advanced Research Centre for Powder Metallurgy and New Materials, Balapur Post, Hyderabad 500 005, India
e-mail: nep@dmrl.ernet.in

Abstract. Aluminium–lithium alloys hold promise of providing a breakthrough response to the crying need for lightweight alloys for use as structurals in aerospace applications. Considerable worldwide research has gone into developing a range of these alloys over the last three decades. As a result, substantial understanding has been developed of the microstructure-based micromechanisms of strengthening, of fatigue and fracture as well as of anisotropy in mechanical properties. However, these alloys have not yet greatly displaced the conventionally used denser Al alloys on account of their poorer ductility, fracture toughness and low cycle fatigue resistance. This review aims to summarise the work pertaining to study of structure and mechanical properties with a view to indicate the directions that have been and can be pursued to overcome property limitations.

Keywords. Aluminium–lithium alloys; lightweight alloys; mechanical properties.

1. Introduction

Substantial improvements in structural efficiency, fuel saving and payload in aerospace can result if the net weight of the structure is reduced considerably. Weight reductions arising from design modifications or enhancements in mechanical properties alone are marginal as compared to what can be achieved by the use of newer materials with lower density (Lewis *et al* 1978; Ekvall *et al* 1982; Lagenbeck *et al* 1987). Lithium is the lightest metallic element. Each unit addition of Li to aluminium offers nearly 3% in density advantage. Moreover, Li enhances the elastic modulus of Al, nearly 6% per unit weight % of Li addition (Sankaran & Grant 1980; Peel *et al* 1984; Westwood 1990). These apart, Al–Li alloys have been found to exhibit superior mechanical properties as compared to the conventional Al alloys in terms of higher specific strength, enhanced resistance to high cycle fatigue, fatigue crack growth and monotonic as well as cyclic fracture at cryogenic temperatures (Welpmann *et al* 1984; Jata & Starke 1986; Peel 1989; Quist & Narayanan 1989; Starke & Quist 1989; Lavernia *et al* 1990; Venkateswara Rao & Ritchie 1992; Wanhill 1994). Further, Al–Li alloys are

technologically more attractive as compared to the newer structural materials such as Ti alloys and composites, which are prohibitively expensive (Westwood 1990; Wanhill 1994). However, these advantages of Al–Li alloys have not still made them a viable alternative due to their low ductility (Lin *et al* 1982; Sanders & Starke 1982, 1989; Gregson & Flower 1985; Vasudevan & Doherty 1987; Webster 1987), inferior low cycle fatigue resistance (Sanders & Starke 1982; Venkateswara Rao & Ritchie 1992; Eswara Prasad *et al* 1996, 1997; Eswara Prasad & Rama Rao 2000) and inadequate fracture toughness not only in the in-plane but also, more significantly, in the through-thickness directions (Jata & Starke 1986; Gregson & Flower 1985; Suresh *et al* 1987; Venkateswara Rao & Ritchie 1989; Lynch 1991; Eswara Prasad *et al* 1993, 1994). These alloys also suffer from a high degree of crystallographic texture and grain fibering, and consequently anisotropy in the mechanical properties (Peel *et al* 1988; Starke & Quist 1989; Eswara Prasad 1993; Eswara Prasad *et al* 1993; Jata *et al* 1998). Presently, considerable efforts are in progress to overcome these property limitations.

The micromechanisms that govern strengthening in Al–Li alloys are akin to those pertaining to the traditional Al alloys. However, the factors responsible for limited ductility and inadequate fracture toughness in these alloys have been found to be unique to some extent. Several microstructural features, such as the nature and volume fraction of the strengthening precipitates, amounts of the co-precipitates that alter the co-planar slip deformation behaviour, width of precipitate free zone (PFZ) and the content, size and distribution of the coarse and angular equilibrium precipitates, have a pronounced effect on the mechanical behaviour of these alloys. These aspects make the Al–Li alloys scientifically interesting.

Several excellent overviews as well as research studies on various aspects of Al–Li alloys are available in the literature. The topics include casting technologies (Adam 1981; Kim *et al* 1987; Chakravorty 1988; Vijaya Singh & Chakravorty 1989; Vijaya Singh 1997), forming and processing methodologies (Wadsworth *et al* 1986; Reynolds & Creed 1987; Meyer *et al* 1987; Mukhopadhyay *et al* 1990a,b), thermo-mechanical treatments and related microstructural evolution (Sankaran & O'Neal 1984; Gregson *et al* 1986; Flower & Gregson 1987; Kulkarni *et al* 1989; Williams & Howell 1989; Banerjee *et al* 1997; Satya Prasad 1999; Satya Prasad *et al* 2000), and welding and other joining technologies (Edwards & Stoneham 1987; Madhusudhan Reddy & Gokhale 1993; Madhusudhan Reddy 1998; Madhusudhan Reddy *et al* 1998). In the present review, some of the other aspects, especially those related to mechanical behaviour of Al–Li alloys are presented and discussed.

2. Chemical composition of Al–Li alloys

Table 1 lists the chemical composition of various Al–Li alloys that have been industrially produced over the past thirty years. The forerunner Al–Li alloy to be developed and used was the Al–Mg–Li–Zr alloy 1420 (Fridlyander *et al* 1967). In this alloy, the beneficial effect of 5·0 wt.% Mg addition on solid solution strengthening and on improved weldability was combined with the advantages of reduced density, enhanced modulus and precipitation hardening provided by 2 wt.% Li addition. Trace addition of almost 0·1 wt.% Zr was made to control recrystallisation and grain growth. Alloy 1420 was used in MIG-29 aircraft fuselage in the form of welded structures in the early 1980's and subsequently applied to passenger aircraft (Sverdlin *et al* 1998).

However, the strength and fracture toughness of the alloy 1420 were not adequate to meet the demands of modern aircraft, even in terms of specific properties. The reasons for poor fracture toughness, apart from those attributable to impurities, were related to shearing of the

Table 1. Chemical composition of various industrial Al–Li alloys.

Aluminium association (AA/Russian ®) designation	Company / country of origin	Chemical composition (wt.%) [balance - Al]							Ref.
		Li	Cu	Mg	Zr	Si	Fe	Other	
1420[N]	Russia	2·0	–	5·0	0·10	0–0·15	0–0·15	–	Fridlyander (1994)
1421[N]	Russia	2·1	–	5·2		0–0·1	0–0·15	0·15 (Sc)	Fridlyander (1994)
1460[N]	Russia	2·0	3·0	–		0–0·1	0–0·1	0·10 (Sc)	Fridlyander (1994)
8090	Alcan & Pechiney	2·2–2·7	1·0–1·6	0·6–1·3	0·04–0·16	0–0·20	0–0·3	–	Starke & Csontos (1998)
2090	Alcoa	1·9–2·6	2·4–3·0	0–0·25	0·08–0·15	0–0·10	0–0·12	–	Starke & Csontos (1998)
2091 (CP274)	Pechiney	1·7–2·3	1·8–2·5	1·1–1·9	0·04–0·16	0–0·20	0–0·3	–	Starke & Csontos (1998)
2095	Martin Marietta	0·7–1·5	3·9–4·6	0·25–0·8	0·04–0·18	0–0·12	0–0·15	0·25–0·6 (Ag)	Starke & Csontos 1998
1441	Russia	1·8–2·1	1·5–1·8	0·7–1·1	0·04–0·16	0–0·1	0–0·1	–	Bird *et al* (2000)

N = nominal compositions

main strengthening phase δ' (Al_3Li) which led to planar slip – an aspect discussed in detail in the next section. Further research was therefore, directed towards compositions that promised additional non-shearable precipitates that would reduce the tendency for planar slip and lead to further hardening of the alloys (Starke *et al* 1981).

As a result of the above, alloys such as AA 8090, AA 2090, AA 2091, 1441, 1460 were developed around the world. In addition to the δ' precipitate, these alloys contained either one or both of the T_1(Al_2CuLi) and S (Al_2CuMg) precipitate, that served to improve fracture toughness of these alloys (Gregson & Flower 1985; Flower & Gregson 1987).

Al–Li alloys have undergone a few more changes in composition in the last ten years. First, the Li content of some of the alloys was brought down to < 2 wt.%. One such alloy, Weldalite-049 (AA 2095), was developed specially for welded fuel tank applications. This alloy contained higher Cu compared to other Al–Li based alloys and derived its strength mainly from the T_1 phase. In this alloy, Li helped improve the specific modulus. The other alloy with lower Li content was the Russian sheet alloy 1441. Reduction in Li (< 2 wt.%) and Zr ($= 0{\cdot}10$ wt.%) contents, combined with controlled rolling, allowed sheets to have fine equiaxed grain morphology, controlled texture and improved in-plane isotropy of properties (Gokhale *et al* 1994a).

More recent compositional changes have mainly focused on trace element additions like Ag, Ce, Y and Sc. Of these, Sc addition has been the most successful in microstructure refinement and improved microstructural stability at high temperatures (Toropova *et al* 1998). Some of the Sc-modified variants of the alloy 1420 are produced commercially in Russia and used widely for welded applications.

3. Microstructure and texture

The properties and performance of Al–Li alloys are sensitive to microstructural features such as (i) size and morphology of the grains, (ii) precipitation of various phases at grain boundary or intragranular precipitates (iii) characteristics of the precipitate free zone (PFZ) and (iv) texture. All Al–Li based alloys are wrought alloys and only those processed through the ingot metallurgy route are considered here because of their industrial importance. Wrought alloys generally follow the process sequence: ingot casting, homogenisation, hot and cold working, solution treatment (with or without natural aging or prestretch) and artificial aging. It will be seen that the final microstructure and texture critically depend on one or more of these process steps.

3.1 *Size and morphology of the grains*

Fine grain size is preferred in Al–Li alloys just as in most structural materials. In addition to the usual strengthening effects, fine grain size restricts piling up of dislocations at grain boundaries resulting from co-planar slip. This helps in improving tensile ductility and fracture toughness of these alloys (Starke *et al* 1981).

The final grain size in a wrought heat-treated alloy is the result of complex interactions between the various processing steps that the alloy is subjected to. In any case, it is almost always desirable to cast ingots with a fine grain size, since castability improves with grain refinement. Conventional methods of grain refinement, viz. TiBAl master alloy additions, have been used. However, partial replacement of Ti in $TiAl_3$ and TiB_2 by Zr reduced their potential as heterogeneous nucleation sites, and led to the development of TiCAl type grain refiner additions (Birch & Cowell 1987). More recently, Sc additions were successfully demonstrated

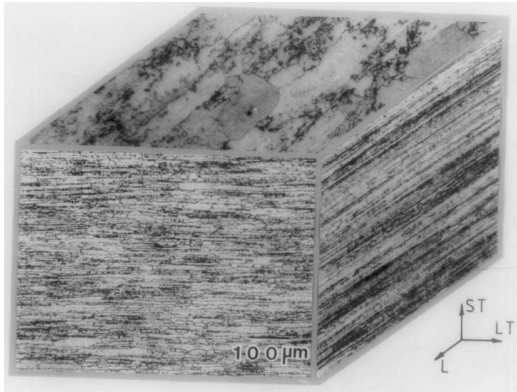

Figure 1. Triplanar optical micrograph of a commercial (Alcan) Al–Li alloy AA 8090 in T8E51 condition, showing wide variation in grain width and aspect ratio in the three orthogonal directions (from Eswara Prasad 1993).

to have a strong grain-refining tendency in Al and Al–Li alloys (Toropova *et al* 1998; Vijaya Singh & Gokhale 2000). Al3Sc particles, having a close crystallographic similarity to α-Al, were shown to be responsible for grain refinement. Higher levels of Zr additions, in the absence of Sc, were also shown to reduce the as-cast grain size. Combined addition of Zr and Sc had a synergistic effect on grain refinement (Vijaya Singh *et al* 2001).

The final grain size and morphology depend upon mechanical working and heat treatment parameters. While dynamic recovery was the most dominant mechanism, dynamic recrystallisation was also observed at very high temperatures and very low strain rates of deformation (Gokhale *et al* 1994b). Most commercially processed wrought products, therefore, show pancake-type grain structure with large variation in grain width and grain aspect ratios in the three orthogonal directions (see figure 1).

Early researchers designed mechanical working and heat treatment processes such that recrystallisation was suppressed, specially in thick products. The unrecrystallised grain structure was shown to result in an improved strength–toughness relationship (Peel *et al* 1988). However, unrecrystallised pancake-shaped grain structure was also found to be associated, due to weak high angle grain boundaries, with poor through-thickness properties and easy delamination after repeated fastening and unfastening operations (Grimes 1990). These problems led to process/alloy modifications that increased the degree of recrystallisation and introduced randomisation of texture (see also § 3·4). The most successful attempt to produce fine recrystallised grain structure has been in case of the Russian alloy 1441 used for damage tolerant, low to medium strength applications (Gokhale *et al* 1994a). Limiting Zr content to 0·08–0·10 wt.% and optimisation of rolling and heat treatment parameters were responsible for producing fine, equiaxed grain structure. Although texture in these alloys is not totally random, the texture components are balanced in such a way that near-isotropic in-plane properties are achieved (Singh *et al* 1999).

Development of plate products with increased degree of recrystallisation was reported in alloys with 1·5 wt.% Li, in which a part of Zr was replaced by Mn (Balmuth & Chellman 1987). However, since the specific modulus of such compositions is not attractive, the usage of these alloys in structural applications is not clear.

3.2 *Precipitation of various phases*

Figure 2 schematically shows various possible phases present in the Al–Li alloy AA8090 in the peak-aged condition. Details of the precipitation reactions, effect of alloy composition

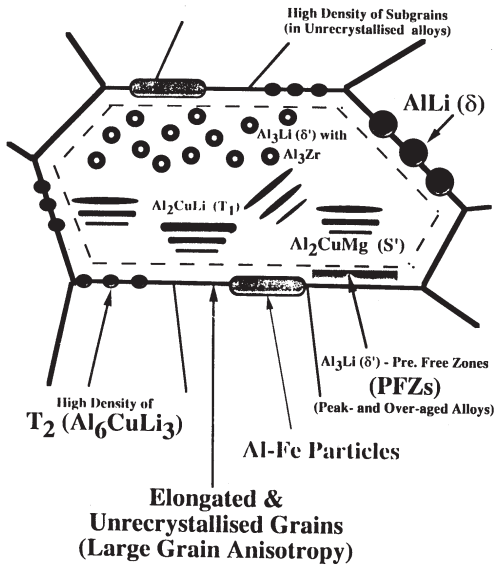

Figure 2. A schematic showing the salient microstructural features of Al–Li alloys AA 8090.

and the characteristics of these phases have been described in literature (Gregson & Flower 1985; Mukhopadhyay 1988; Sanders & Starke 1989; Satya Prasad 1999).

The as-cast microstructure contains various intermetallic phases originating from impurity elements such as Fe, Si and constituent particles due to non-equilibrium solidification. The impurity phases are highly stable and continue to be present even in the final product. On the other hand, a well-designed homogenisation treatment can dissolve most of the constituent particles (Gokhale & Ramachandran 1990).

The behaviour of Zr is somewhat different. Under typical casting conditions and Zr content within the specified limits of commercial alloys, Zr remains dissolved in a supersaturated condition in α-Al. During homogenisation, precipitation of metastable Al_3Zr (β', having $L1_2$ superlattice structure) occurs, beginning around 350°C. After typical homogenisation treatment at 535°C for 24 h, a non-uniform distribution of 20–30 nm size Al_3Zr precipitates is present (Satya Prasad 1999). These Al_3Zr precipitates are spherical and fully coherent with a cube–cube orientation relationship with α-Al. Scandinium is also known to behave in a similar manner as Zr and forms Al_3Sc particles during homogenisation (Toropova *et al* 1998). $Al_3(Sc_xZr_{1-x})$ precipitates form in alloys that contain both Zr and Sc. $Al_3(Sc_xZr_{1-x})$ phase has $L1_2$ crystal structure and forms spherical precipitates during homogenisation (Satya Prasad *et al* 2001).

Cooling of the ingots from the homogenisation temperature and subsequent thermomechanical processing invariably results in the precipitation of equilibrium phases such as Al_6CuLi_3 (T_2) and AlLi (δ). Details of the size, distribution and orientation relationships of the equilibrium precipitates that form during sub-solidus temperature exposure are described in the literature (Satya Prasad 1999). These precipitates can play an important role in the processing of sheet products that are to be formed superplastically (Wadsworth *et al* 1984). For the conventional structural applications, the equilibrium precipitates are taken back in solution during the subsequent solutionising treatment, and the response to age hardening treatments depends critically on the successful desolution of these equilibrium precipitates.

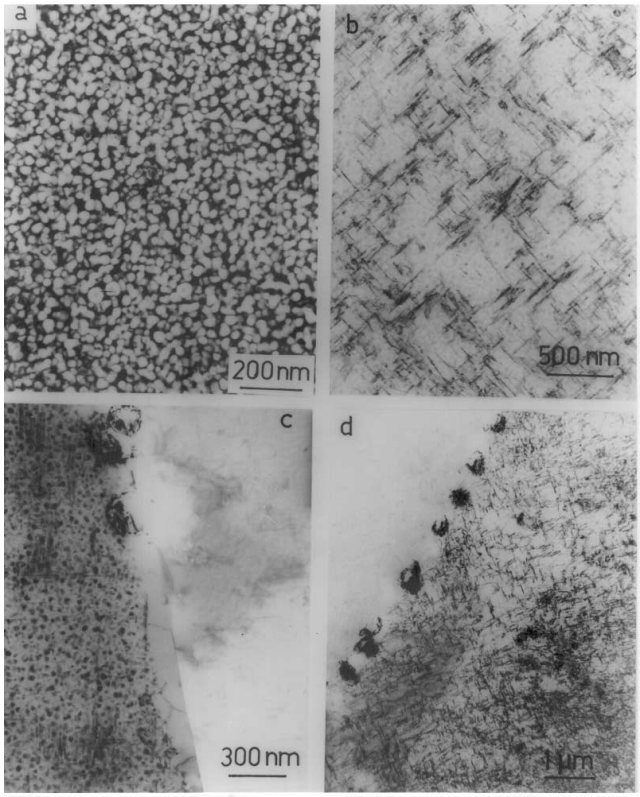

Figure 3. Transmission electron micrographs of AA 8090-T8E51 alloy plate showing **(a)** distribution of δ' precipitates, **(b)** distribution of S precipitates, **(c)** δ'-precipitate free zones, and **(d)** network of T_2 (Al_6CuLi_3) precipitates along the high angle grain boundary.

In addition to the equilibrium precipitate desolution, the solution treatment can alter the nature of the metastable β' precipitates. Recent work shows that recrystallisation can change the morphology of β' precipitates from spherical to a facetted one (Satya Prasad *et al* 1999). The cube–cube orientation relationship of the spherical precipitates changes to a twin relationship on facetting. Similar changes in the nature of β' precipitates were observed in unrecrystallised alloys, but were restricted to regions close to the grain boundaries. In both cases, facetting was related to the particle–grain boundary interaction.

Aluminium–lithium alloys are typically aged at 150 to 190°C. δ' is the most dominant phase that precipitates readily on aging at these temperatures or even at room temperature (natural aging). δ' has $L1_2$ superlattice structure and a cube–cube orientation relationship with α-Al. It precipitates either homogeneously or heterogeneously enveloping spherical β' precipitates forming the characteristic bull's eye structure (see figures 2 and 3a). $Al_3(Sc_xZr_{1-x})$ particles also participate in the heterogeneous nucleation of δ' (Balabhaskaran *et al* 1999). Evidence of superlattice reflections in as-solution treated alloys suggests that δ' forms during solution treatment also. The natural aging phenomenon limits the duration of room temperature storage of solution treated semiproducts before stretching, forming etc. (Grimes 1990).

In addition to the uniformly and densely distributed δ', artificially aged Al–Li alloy AA8090 also contains a reasonable amount of lath-shaped, semi-coherent precipitates of orthorhombic Al_2CuMg (S or S') phase. Precipitation of S' is initially slow due to the unavailability of adequate concentration of vacancies which have a high binding energy with Li atoms. Prior natural aging or 2–3% tensile prestretch before artificial aging or overaging accelerates the

S or S' precipitation (Flower & Gregson 1987). In addition to δ' and S', sparsely distributed plates of Al_2CuLi (T_1) precipitates, having a hexagonal crystal structure are also present in many Al–Li alloys including the AA8090 alloys (see the TEM micrographs in figure 3). In Mg-free alloys, such as AA2090, S precipitates are absent and, in these alloys T_1 is the second major phase. In the Cu-free alloys of 1420 family, δ' is the only metastable phase present (Eswara Prasad *et al* 1991).

Aging to near-peak or beyond peak hardness can cause precipitation of equilibrium phases T_2 or δ (Satya Prasad *et al* 2000). The preferred sites for nucleation are grain boundaries, the α-faceted β' interface (for T_2) and α-T_2 interface (for δ). Unaided precipitation of T_2 within the grains has been observed after longer aging times. It is interesting to note that the two forms of β' precipitates nucleate two different types of precipitates δ' on spherical β' and T_2 on faceted β'. TEM observations of Li-rich equilibrium phases has posed several challenges due to attack from electropolishing media.

3.3 *Precipitate free zones (PFZs)*

Another significant aspect of microstructure in Al–Li based alloys, as in high strength Al–Zn–Mg based alloys, is precipitate-free zones (PFZs). In peak- and over-aged alloys, regions of about $0{\cdot}5\ \mu$m wide neighbouring grain boundaries and equilibrium precipitates are found to be free of δ' precipitates (Starke *et al* 1981). These zones are shown to form due to the depletion of Li, associated with the formation of Li-rich equilibrium phases (Radmilovic *et al* 1989). Although strain localisation at a soft PFZ has been identified in many systems and seems likely to promote grain boundary ductile fracture at the grain boundary precipitates, no direct experimental confirmation of embrittlement by PFZ strain localisation has yet been found (Vasudevan & Doherty 1987). However, the changed electrochemical nature in the grain boundary regions makes them more prone to various forms of localised corrosion (Bavarian *et al* 1989).

The PFZ was shown to grow parabolically with time for a given Li content and aging temperature (Jha *et al* 1987). The formation of PFZ is essentially a diffusion-controlled process; hence, increasing aging temperature accelerates PFZ formation. Higher Li contents increase PFZ width, possibly because of higher inter-diffusion coefficient (Jha *et al* 1987). Underaging is preferred, in general, to minimise PFZs and to prevent coarse equilibrium phase precipitation. A controlled stretch prior to aging then becomes essential to accelerate precipitation of other phases such as S and T_1 to bring the yield strength to those of the peak-age levels. Figure 3c shows a typical PFZ in an AA8090 alloy.

3.4 *Crystallographic texture*

All high strength aluminium alloy wrought products are prone to the formation of crystallographic texture (Palmer *et al* 1986). The effects are greatest in unrecrystallised products, although recrystallised texture may be strongly related to the unrecrystallised texture (Balmuth 1994; Engler *et al* 1996; Hales & Hafley 1998). Presence of intense texture has strong effects such as: at least 15% lower yield strength and higher fatigue crack growth rates at 45–60° from the working direction, low fracture toughness and bend ductility in the working direction, and variation in elastic properties (Warren & Rioja 1989; Eswara Prasad & Malakondaiah 1992; Balmuth 1994; Jata *et al* 1996). Variability in texture through the thickness in plate, and variations in extrusion shape result in further variability of these properties (Sanders & Starke 1989).

Hot rolling Al–Li alloys was shown to result in the formation of texture, dominated by Bs $\{110\}\langle 112\rangle$ or 'brass' component (Gregson & Flower 1985). In hot extruded plates, significant

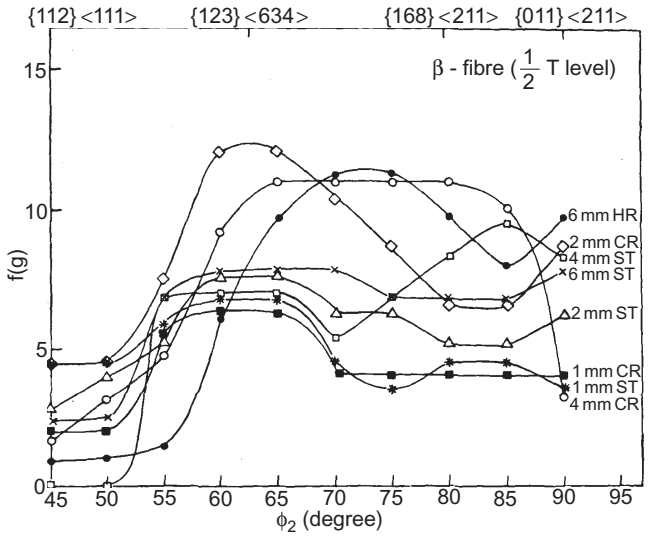

Figure 4. Intensities of various texture components at half thickness level for an AA 8090 alloy processed to various stages by hot rolling (HR), cold rolling (CR) and solution treatment (ST). Major texture components such as copper $\{112\}\langle 111\rangle$, $S\{123\}\langle 634\rangle$, brass $S\{168\}\langle 211\rangle$ and brass $\{011\}\langle 211\rangle$ have been indicated.

amounts of Bs, S $\{123\}\langle 634\rangle$ and Cu $\{112\}\langle 111\rangle$ components were observed (Jata *et al* 1998). Cross-rolling introduced strong component of Bs/S $\{168\}\langle 211\rangle$ texture (Singh *et al* 1998). Retention of texture components after solution treatment depends up on the hot/cold working parameters as well as annealing conditions (Palmer *et al*1986; Jata *et al* 1998). For example, lower extrusion temperatures were shown to eliminate most Bs component after solution treatment (Jata *et al* 1998). Similarly, multiple cold rolling followed by solution treatments significantly reduced the Bs component in AA8090 type Al–Li alloys (see figure 4) (Singh *et al* 1998). The in-plane tensile property anisotropy was shown to be strongly influenced by the intensity of the Bs texture component, thus suggesting directions for further process optimisation to improve in-plane isotropy in properties (Jata *et al* 1996). Other approaches, including trace additions of Mn, were also shown to reduce the intensity of texture in plate products (Balmuth 1994). Another commonly used method to encourage recrystallisation (and therefore, reduce texture) is to rapidly heat sheet products to the solutionising temperatures using salt baths (Gokhale *et al* 2000).

4. Strengthening mechanisms and planar flow deformation

Contributions from various classical strengthening mechanisms in Al–Li alloys have been assessed (Fragomeni *et al* 1989). The precipitation hardening associated with the δ' is found to be the most dominant one (nearly 50–60 % or even more). The roles of different phenomena that actually result in precipitation strengthening are also discussed in the literature. Order strengthening is also considered to be a significant factor.

Plastic deformation is accompanied by shearing of δ' precipitates, which in turn results in co-planar slip, a phenomenon considered responsible for low ductility, inadequate fracture toughness and inferior low cycle fatigue resistance in these alloys. Dislocations can cut/shear these ordered, strengthening precipitates below a critical size or loop around the bigger sized precipitates. Orowan looping was found to be predominant only when the δ' size is in excess of 30 μm in radius (and a corresponding mean interparticle spacing in excess of 100 μm),

below which particle shearing dominates (Miura *et al* 1989). It is widely agreed now (Palmer *et al* 1986) that strengthening in the particle shearing regime arises from the creation of anti-phase boundaries (APBs). In order to eliminate the extra energy required to create an APB, dislocations move in pairs such that the order disturbed by the first dislocation is restored by the second. The critical resolved shear stress (τ_{CRSS}) for such a process is given by (Palmer *et al* 1986):

$$\tau_{CRSS} \alpha (\gamma_{APB})^{3/2} f^{1/2} r^{1/2}, \tag{1}$$

where γ_{APB} is the APB energy of the δ' precipitates, f is their volume fraction and r the radius. The ordered precipitate would have reduced strength due to the reduction in the cross-sectional area once it is sheared. If n_d number of dislocations, each with a Burger's vector of b_v shear a given particle, assuming that the shearing occurs along the diameter, then the τ_{CRSS} for further shearing would become,

$$\tau_{CRSS} \alpha (\gamma_{APB})^{3/2} f^{1/2} (r - n_d b_v)^{1/2}. \tag{2}$$

The reduction in τ_{CRSS} is significant with particle shearing and further slip on the same plane becomes easier. Hence, slip becomes co-planar and the particular slip plane on which the repeated shearing occurs becomes work softened. The Al–Li alloys, aged to near peak strength and beyond, exhibit such co-planar slip extensively and this mechanism is primarily responsible for lower ductility and lower fracture toughness.

Two approaches have been made to ameliorate the detrimental effects of co-planar slip. First, co-precipitation of phases that do not undergo shearing easily (simultaneous additions of Cu and Mg, resulting in S or S' precipitates or Mn additions resulting in incoherent Al_6Mn precipitates) has been used in reducing the co-planarity (Balmuth & Chellman 1987). Secondly a smaller grain size is preferred, since it reduces length of the dislocation pile-up that can form at high angle grain boundaries (Starke *et al* 1981). In spite of these remedial measures, slip co-planarity occurs, manifested as steps on grain boundaries exposed to the fracture surface. This situation is attributable to the fact that commercial tempers tend to be in underaging regimes for the sake of other property advantages, with inadequate amount of S phase (Gokhale *et al* 1994a).

5. Tensile deformation and anisotropy

Typical tensile load (stress)–strain curves for Al–Li based alloys are shown in figure 5. Serrated yielding, and the related co-planar slip, is seen to be present in underaged alloys. Failure generally occurs at peak stress in most of the Al–Li alloys, except when ductility is high (see figure 5b).

Tensile properties of a few quaternary alloys are given in tables 2 and 3. The properties depend upon (a) the type of semi-finished product and (b) test direction with respect to the principal direction of mechanical working. Extruded products usually show maximum strength (in the longitudinal, L direction) among various semi-finished products. Plates have intermediate strengths, while sheet products generally have lower strengths. The differences in tensile properties are related to the extent of mechanical or grain fibering (highest in extrusions) and degree or recrystallisaiton, apart from the nature and intensity of the crystallographic texture. Mechanical fibering increases strength in the fibre direction, though properties in the other directions tend to be lower. Recrystallisation lowers overall tensile properties due to loss of the substructure.

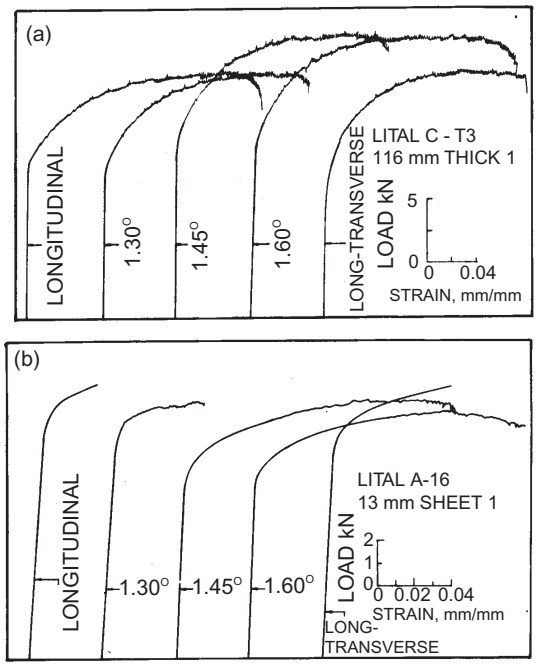

Figure 5. Load–strain plots of AA 8090 Al–Li alloys in **(a)** underaged (Lital C-T3) and **(b)** peakaged (Lital A–T6) conditions. Except for L and LT directions in the peak-aged alloy, in the other conditions the alloys exhibit serrated yielding and co-planar slip (from Eswara Prasad & Malakondaiah 1992).

Table 2. Tensile properties of Al–Li alloy plate products.

Alloy	Plate thickness (mm)	Direction	0·2% PS (MPa)	UTS (MPa)	Elongation (%)	Ref.
8090-T8	6–38	L	405	462	6·3	Gatenby *et al* (1989)
		LT	360	462	7·1	
	38–65	L	397	449	5·6	
		LT	354	447	7·5	
		ST	288	421	5·6	
8090-T8 (DMRL)	25	L	409	466	8·2	Singh & Gokhale (2000)
		L-45°	375	447	8·0	
		ST	319	391	2·6	
	50	L	381	454	9·2	
		ST	341	437	5·6	
2024-T351	6–38	L	366	473	18	Gatenby *et al* (1989)
		LT	331	475	16	
	38–65	L	365	470	17	
		LT	335	472	15	
		ST	298	414	5·8	

L: longitudinal; LT: long-transverse; ST: short-transverse; L-45°: 45° to the longitudinal direction

Table 3. Properties of Al–Li and other aircraft grade Al-alloy sheets.

Alloy	Temper	Product form	Direction	0·2% PS (MPa)	UTS (MPa)	Elongation (%)	Ref.
8090[t]	T8	Sheet (3 mm)	L	415	523	7·5	Grimes (1990)
			LT	408	508	4·0	
			L-45°	338	431	13·5	
1441[t]	T8	Sheet (3 mm)	L	399	456	9·2	Gokhale *et al* (1994)
			LT	423	482	8·8	
			L-45°	392	462	10	
8090 (DMRL)	T8	Sheet (2–4 mm)	L	404	475	6·0	Gokhale *et al* (1998)
			LT	416	487	7·0	
			L-45°	377	460	9·1	
1424 (Contains Sc)	#	Sheet (1·6 mm)	L	360	515	8	Fridlyander *et al* (1998a)
			LT	370	520	16	
			L-45°	295	470	26	
1421 (Contains Sc)	#	Sheet (2·5 mm)	L	360	469	8	Fridlyander *et al* (1998b)
			LT	380	500	10	
			L-45°	339	470	15	

Air quenched from solutionising temperature + 3-stage aged; t – typical properties

One of the major problems associated with Al–Li alloys is anisotropy in tensile properties, which in turn, governs the extent of anisotropy in the other mechanical properties (Eswara Prasad & Malakondaiah 1992; Eswara Prasad 1993). Low yield strength at intermediate test directions, i.e., 45–60° to the rolling direction in case of plates and sheets, with respect to the principal direction of mechanical working, is the most prominent manifestation of the anisotropy. This is related to the development and retention of crystallographic texture (Jata *et al* 1998). Another form of anisotropy is the poor short-transverse ductility, particularly in thick products like plates. This is related (i) to the pancake grain structure that is generally present in such products, (ii) to the presence of some strengthening precipitates and (iii) to the presence of weak high and/or low angle grain boundaries and the associated weakening features such as coarse equilibrium particles and precipitate free zones (Jata *et al* 1998). Attempts have been made to induce recrystallisation through modifications in the alloy composition and the processing parameters to impart adequate degree of isotropy in properties (Gokhale *et al* 1994a; Singh *et al* 1999).

Two more such successful attempts have involved use of overaging and rapid heating to the solutionising temperature. Gregson & Flower (1985) have shown that overaging in case of quaternary Al–Li–Cu–Mg alloys results not only in improving tensile ductility of the alloy but also provides improved isotropy in tensile properties (see figure 6). It is noteworthy to observe from the data in figure 6 that the enhanced isotropy thus obtained occurs without any

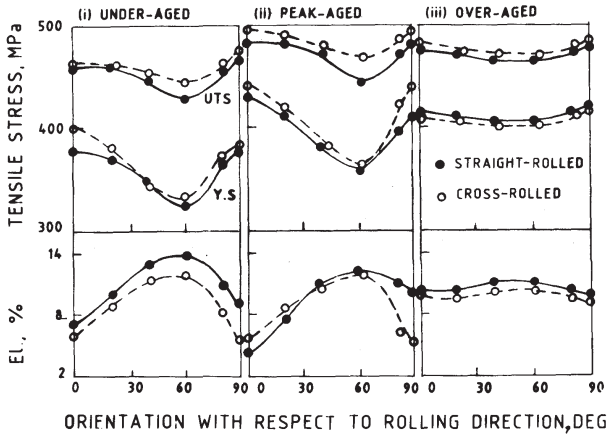

Figure 6. Variation of tensile properties with orientation with respect to the rolling direction. The data show considerable isotropy in the overaged condition (from Gregson & Flower 1985).

significant reduction in the strength levels. The beneficial effects are again attributed to the copious amounts of *S* phase precipitates, which essentially cause slip homogenisation. The second methodology which imparts isotropy is rapid heating to the solutionising temperatures using 'salt baths' (Clarke *et al* 1986; Reynolds *et al* 1986). The salt bath treatments result in more favourable precipitate distribution and reduction in the propensity of crystallographic texture (see figure 7)

More work is required however, to understand the development and effect of texture on the mechanical property anisotropy in these alloys. There is evidence, e.g. that property isotropy can be improved by employing certain types of not necessarily randomized textures (Singh *et al* 2001).

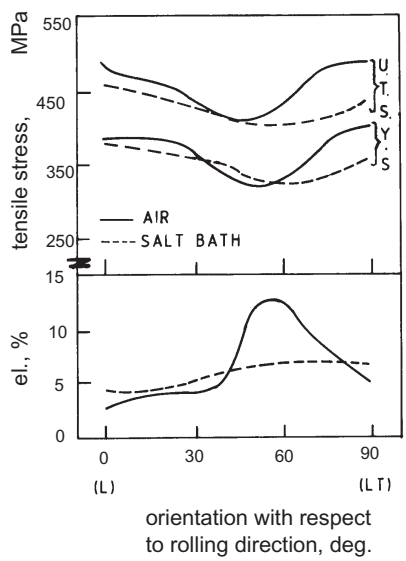

Figure 7. Variation in tensile properties with respect to the rolling direction. The alloy, heat treated using salt bath shows higher degree of isotropy, especially tensile elongation (from Reynolds *et al* 1986).

6. Low cycle fatigue

Low cycle fatigue (LCF) resistance of several Al–Li alloys has been evaluated (Sanders & Starke 1982; Srivatsan & Coyne 1986; Srivatsan *et al* 1986; Venkateswara Rao & Ritchie 1992; Eswara Prasad *et al* 1992, 1994, 1996, 1997; Eswara Prasad & Rama Rao 2000). These and several other studies have dealt principally with (i) LCF resistance and the factors that affect LCF resistance, (ii) anisotropy in LCF resistance, particularly in the plate or bar product forms and finally (iii) micromechanisms responsible for the observed bilinearity in fatigue life variation with LCF damage parameter. Each of these aspects has significant technical importance in the design and development of components that undergo plasticity-controlled fatigue deformation, damage and failure. Further, most of the Al–Li alloys, when evaluated over a reasonably wide range of plastic strain amplitude, exhibit bilinear nature of power-law relationship with two sets of power-law constants, one set corresponding to the lower strain amplitudes, below the transition called 'hypo-transitional region' and the other set corresponding to the higher strain amplitudes, above the transition called 'hyper-transitional region'. It is important to note that factors for such bilinearity are found to affect equally the other two aspects of LCF of these alloys, viz. fatigue resistance and anisotropy in the fatigue resistance. This section is devoted to a discussion of these aspects.

6.1 *Low cycle fatigue resistance*

Several studies conducted so far on Al–Li alloys indicate that these alloys exhibit inferior high-strain, low-cycle fatigue (LCF) resistance when compared to the other structural Al alloys (Starke & Sanders 1982; Venkateswara Rao & Ritchie 1992; Eswara Prasad & Rama Rao 2000). The factors that contribute to the low values of tensile ductility and inadequate fracture resistance are also responsible for the inferior LCF resistance in these alloys – the principal contributing micromechanism being co-planar deformation and the resulting strain localisation along the high angle grain boundaries (Starke & Sanders 1982; Srivatsan *et al* 1986; Eswara Prasad *et al* 1996).

Figures 8 and 9 present fatigue life data, as a function of plastic strain amplitude (or hysteresis energy ΔW_p as in figure 8) for several Al–Li alloys, also a few commercial Al alloys. The effect of alloy composition and aging treatment on LCF resistance is evident in the figure 8 which follow the bilinear Coffin-Manson (C-M) power law relationship.

6.1a *Effect of alloy composition:* In a systematically conducted study on pure Al and Al–Li binary alloys with varied Li content, Dhers and co-workers (1986) have shown that Li in solid solution of aluminium (weight % Li < 0·7) does not affect LCF resistance significantly. On the other hand, further additions of Li (weight % Li > 1·1) which result in copious precipitation of ordered, coherent δ' (Al_3Zr), decreases LCF resistance markedly. These authors have shown that LCF resistance of binary Al-2·5wt.%Li is nearly two orders of magnitude, in terms of C–M relationship, lower than the pure Al and Al-0·7wt.%Li solid solution alloy. Such drastic reduction in LCF resistance was attributed to pronounced strain localisation through δ'-precipitate shearing and the resultant intergranular fracture. Manganese added as grain refiner does not improve LCF, though it enhances the strength of the binary alloy (Coyne *et al* 1981). However, major alloying additions of Cu, with or without Mg improves LCF resistance substantially with nearly the same or in some cases with improved tensile strength.

As shown in figure 9, the thermo-mechanically treated, ternary Al–Cu–Li (AA 2020) and quaternary Al–Li–Cu–Mg (AA 8090) alloys show LCF resistance that is nearly an order of

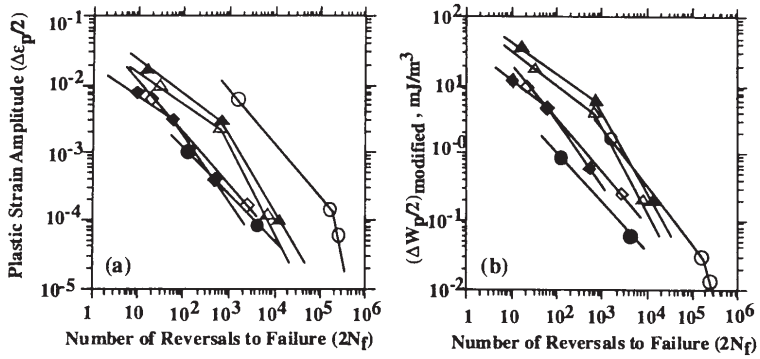

Alloy	Symbol	Power-law constants			
		ε_f'	$-c$	W_f^*, MJ/m^3	$-\beta^*$
Al-2·5 wt.% Li (UA)					
Hypo-transition		$>10^3$	2·38	$>10^5$	2·31
Hyper-transition		2·1	0·8	811	0·85
Al-2·5 wt.% Li (PA)		0·032	0·71	36·1	0·77
Al-3 wt.% Li+Mn (UA)		0·059	0·76	85·1	0·74
Al-3 wt.% Li+Mn (PA)					
Hypo-transition		0·15	0·96	220	0·96
Hyper-transition		0·021	0·48	37	0·52
AA 8090-T3-L					
Hypo-transition		4·07	1·17	8797	1·19
Hyper-transition		0·05	0·48	92·7	0·49
AA 8090-T8E51-L					
Hypo-transition		5·5	1·15	11118	1·15
Hyper-transition		0·06	0·46	127	0·47

Figure 8. Effect of degree of aging in Al–Li alloys of three different compositions. For the details of the power-law constants given in the accompanying table, please refer to Eswara Prasad & Rama Rao (2000). The variation of fatigue life is considered with respect to the plastic strain amplitude ($\Delta\varepsilon_p/2$) in **(a)** and average plastic strain energy per cycle (ΔW_p) in **(b)**.

magnitude higher than that of the binary Al–Li alloys. LCF resistance of these alloys form the upper band among the several Al–Li alloys studied till date. The improved microstructural condition namely the nearly unrecrystallised grain structure, obtainable by a novel thermo-mechanical treatment in a AA 2020 (Srivatsan *et al* 1986) and the presence of copious amounts of slip homogenisor, S' (Al_2CuMg), obtainable by a tensile pre-stretch in the solution-treated condition before the final aging in a partially recrystallised AA 8090 alloy (Eswara Prasad *et al* 1996), are primarily responsible for the improved LCF resistance. Both these microstructural conditions suppress intergranular fracture to a large extent and promote the high energy transgranular shear fracture. These studies have further shown that the ternary and the quaternary alloying additions result not only in improved LCF resistance but also in increased strength of Al–Li alloys.

6.1b *Degree of aging:* In case of the binary Al-2·5 wt.%Li alloy, an increase in the degree of aging (as defined by Suresh *et al* 1987) decreases LCF resistance (see figure 8). Fatigue lives at any particular plastic strain amplitude are nearly two orders of magnitude lower in the peak-

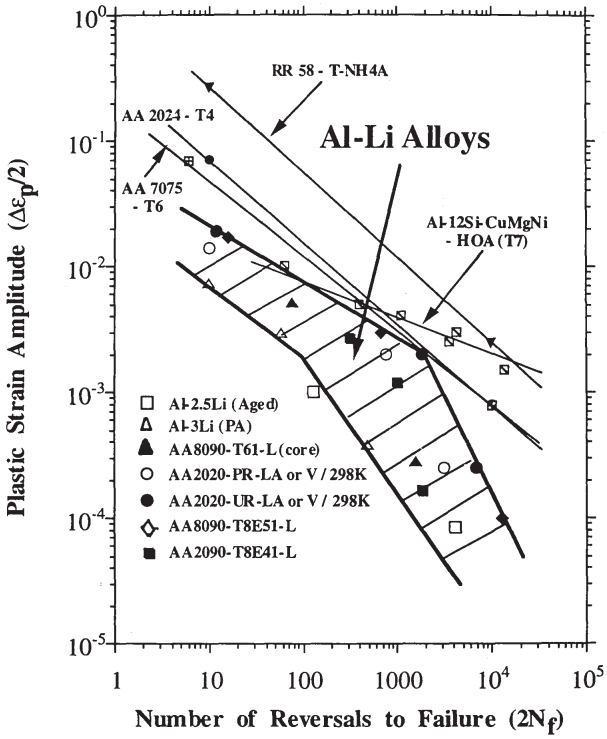

Figure 9. Comparison of LCF resistance of Al–Li alloys with that of traditionally used aircraft structural Al alloys, based on plastic strain amplitude (Dep/2) (from Eswara Prasad & Rama Rao 2000).

aged alloy as compared to the under-aged condition (Dhers *et al* 1986). Such sharp decrease in LCF resistance has been attributed to the combined effects of increased degrees of planar flow that occurs with the δ' precipitate coarsening and grain boundary brittleness due to the precipitation of coarse and columnar δ (Al–Li) at the high angle grain boundaries. However, the effect of degree of aging on LCF resistance is not always detrimental. Eswara Prasad *et al* (1997) have shown that in case of the AA 8090 Al–Li alloy, an increase in the degree of aging increases LCF resistance (see figure 8). Such beneficial effects have been attributed to the combined effects of higher amounts of unrecrystallised grains of the peak-aged alloy and the enhanced S¢ precipitation that occurs with increase in degree of aging. In a third study, Coyne *et al* (1981) have shown that the effect of degree of aging is marginal – possibly the beneficial effects of coprecipitation are almost normalised with the detrimental effects of grain boundary brittleness.

In all these studies, grain refinement and often the complete suppression of recrystallisation resulting in near- or fully-unrecrystallised grain structure has been found to be beneficial in improving LCF resistance. Such microstructural modification is obtained either by novel thermomechanical treatments (Srivatsan *et al* 1986) or by the use of higher content of grain refining elements, such as zirconium (Flower & Gregson 1987). The fatigue lives of the unrecrystallised grain structured alloys are nearly 2 to 3 times higher, at any particular plastic strain amplitude, as compared to their recrystallised counterpart (Srivatsan *et al* 1986). However, the use of unrecrystallised grain structured alloys has to be viewed with caution as such a stratagem also results in higher degree of anisotropy, both in in-plane and in through-thickness directions – an aspect discussed in the next section.

6.2 *Anisotropy in the LCF properties*

Aluminium–lithium alloys exhibit anisotropy in the LCF properties, although to a lesser degree as compared to that observed in tensile properties (Khireddine *et al* 1989; Eswara Prasad *et al* 1989, 1996; Eswara Prasad 1993). The extent of the anisotropy in both tensile and fatigue properties is such as to warrant due consideration while designing components from these alloys. Anisotropy occurs because of a strong crystallographic texture and grain fibering. Factors which are responsible include grain structure, directionality in shearability of the major strengthening precipitates, δ' and T_1, alignment of high and low angle grain boundaries and the distribution of the coarse, angular grain boundary precipitates. While crystallographic texture governs anisotropy in the cyclic stress response behaviour and the cyclic strength coefficient, the grain fibering characteristics were found to affect significantly the nature of deformation, fracture mode and the number of cycles to failure (life) under LCF conditions.

Studies on anisotropy in the LCF behaviour (Khireddine *et al* 1989; Eswara Prasad 1993; Eswara Prasad *et al* 1996) have shown that the nature of cyclic stress response in the quaternary Al–Li–Cu–Mg alloys is similar in the through-thickness and in-plane directions. Anisotropy is evident in terms of the values of the stress amplitudes and the extent of cyclic hardening and softening in the different test directions. Anisotropy in fatigue lives and cyclic ductility closely follow the trends in tensile ductility in the higher strain amplitude region and the same in the lower strain amplitude region are found to be dependent on alloy chemistry and processing history. A comparison of the results from these studies has shown that anisotropy in the LCF properties is far more pronounced in the through-thickness direction as compared to the in-plane orientation. The fatigue lives at any particular strain amplitude are up to 200% higher in the longitudinal sections of the core of the extruded bar as compared to those in the long-transverse direction of the core section or the longitudinal direction of the surface section (Khireddine *et al* 1989). The values of cyclic ductility too are more than 350% higher in the longitudinal direction of the core section as compared to the other two test directions. The degree of anisotropy in LCF properties is less pronounced in the in-plane orientation, which has been evaluated in case of a cross-rolled plate (Eswara Prasad *et al* 1996). Fatigue resistance in this plate, measured in terms of cycles to failure at a particular strain amplitude, is only 60–120% higher in the long-transverse direction as compared to the longitudinal and L + 45° (stress axis is at 45° to the rolling direction) directions.

6.3 *Bilinearity in the power law relationships*

Most of the Al–Li alloys evaluated till date exhibit bilinearity in the fatigue power-law relationships, an aspect which was studied in detail by the present authors (Eswara Prasad 1993; Eswara Prasad *et al* 1989, 1994, 1996, 1997; Eswara Prasad & Rama Rao 2000). The bilinearity is evident in terms of the two different linear relationships with different power-law constants in the two regions of the variation in the fatigue life (represented by the number of reversals to failure) with respect to a particular fatigue damage parameter. Depending upon the damage parameter considered, these power-law relationships are known as Coffin–Manson relationship which is based on the plastic strain amplitude ($\Delta\varepsilon_p/2$), Basquin-like relationship, based on the average stress amplitude ($\Delta\sigma/2$) or the Halford–Morrow relationship, based on the average plastic strain energy per cycle (ΔW_p). Bilinearity in these power-law relationships assume importance as the fatigue resistance estimated at a particular value of $\Delta\varepsilon_p/2$ or $\Delta\sigma/2$ or ΔW_p, derived from the extrapolations made in the one of the two regions, grossly overestimates fatigue resistance in the other region (Eswara Prasad *et al* 1997). Apart

from this, the micromechanisms that contribute to the fatigue damage are found to be different for the two regions, namely the hypo-transition region (below the transitional value) and the hyper-transitional region (above the transitional value). The determination of these operating micromechanisms not only leads to an understanding of the causes for the observed bilinearity, but also it provides the means for the improvement of LCF resistance.

Based on the compilation of results from several studies, Eswara Prasad *et al* (1996) have concluded that the three principal mechanisms that generally contribute to the bilinearity in structural alloys are operational in Al–Li alloys as well. These are (i) change in the nature of deformation-either homogenous or heterogeneous slip, detected through transmission electron microscopic observations (Srivatsan & Coyne 1986, 1987; Srivatsan *et al* 1986; Khireddine *et al* 1989; Eswara Prasad *et al* 1994, 1996; Oh *et al* 1999) or the variation of cyclic work hardening exponent, n' (Eswara Prasad *et al* 1989, 1996), (ii) change in the deformation-assisted fracture mode (Heikkenen *et al* 1981; Sanders & Starke 1982; Srivatsan *et al* 1991; Eswara Prasad *et al* 1989, 1996; Oh *et al* 1999) and (iii) change in the environment assisted fracture mode (Sanders & Starke 1976; Eswara Prasad *et al* 1994, 1996).

In case of Al–Li alloys, which are principally strengthened by the semi-coherent θ' (Al_2Cu) precipitates, the nature of deformation changes from a highly heterogenous co-planar slip with considerable precipitate disordering and shearing after continuous to and fro motion of dislocations through the precipitates (causing considerable precipitate disordering) at the lower strain amplitudes to a highly homogeneous, multiple slip at higher strain amplitudes (Srivatsan *et al* 1986). The co-planar slip which occurs on a single preferred slip plane results in strain localisation, which in turn results in low energy intergranular fracture at these lower strain amplitudes (hypo-transitional region). Additional contributions from the higher extent of environmental assisted fracture during long fatigue lives, have a supplementary effect as both tests conducted in laboratory air atmosphere and vacuum environment have shown the same fracture morphology of intergranular fracture in the hypo-transitional region. On the other hand, homogenous deformation due to active slip on many slip planes results in higher energy transgranular fracture at the higher strain amplitude hyper-transitional region. These results are similar to the studies reported widely in case of nimomic alloys strengthened by the semi-coherent γ' precipitates (Sundararaman *et al* 1990; Singh *et al* 1991). On the other hand, in case of the δ'-precipitate (fully-coherent with the matrix α-Al) strengthened Al–Li alloys, the nature of change in the deformation and deformation-assisted fracture is opposite to the above. In this case the δ'-precipitate shearing occurs once a critical resolved shear stress exceeds a particular value and further slip on the same slip plane results in co-planar slip at higher stress amplitudes or the corresponding higher strain amplitudes. The associated precipitate disordering is negligibly small. Such co-planar slip results in low energy intergranular fracture at higher strain amplitudes. On the other hand slip at lower strain amplitudes does not cause any precipitate shearing as stresses are well below the critical resolved shear stress. Slip in this situation is locally active and results in dislocation veins or cells with high dislocation density (Khireddine *et al* 1989; Eswara Prasad *et al* 1994, 1996). Such homogeneous deformation results in formation of matrix microcracks which subsequently result in high energy transgranular fracture (Eswara Prasad *et al* 1989, 1994, 1996). Again a significant contribution to fatigue damage can arise from environmental degradation, the extent of which is higher at lower strain amplitudes (Eswara Prasad *et al* 1994, 1996). All these effects are summarised in figures 10 and 11. With the help of such data compilation, Eswara Prasad & Rama Rao (2000) have shown that fatigue degradation in structural alloys in general and Al–Li alloys in particular occurs due to mechanical fatigue, strain localisation through precipitate shearing or disordering, environmental degradation and the differential strain localisation along high angle grain boundaries.

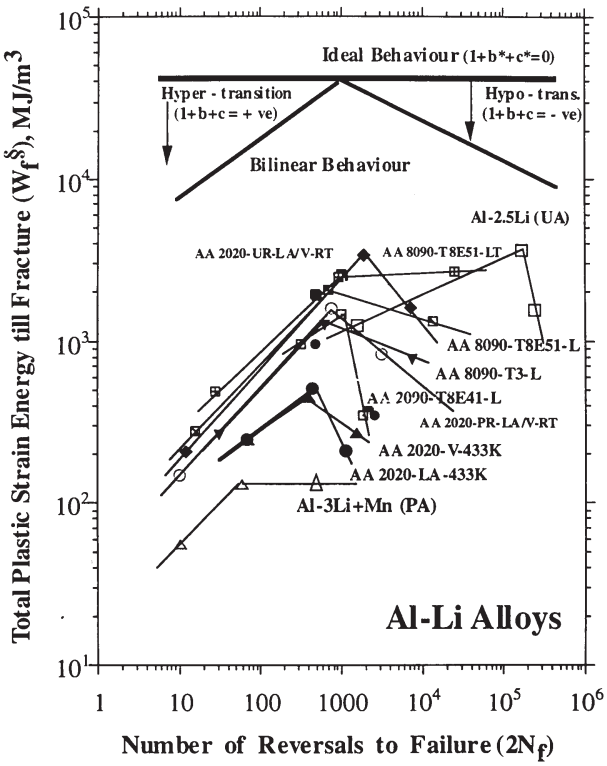

Figure 10. Variation of total cyclic plastic strain energy till fracture $W_f^{\S}$ with number of reversals to failure $2N_f$ for various Al–Li alloys: note that with exception of Al-3wt.%Li + Mn and AA 8090– T8E51 in LT direction, all other alloys exhibit bilinear behaviour shown schematically at the top of figure (from Eswara Prasad & Rama Rao 2000).

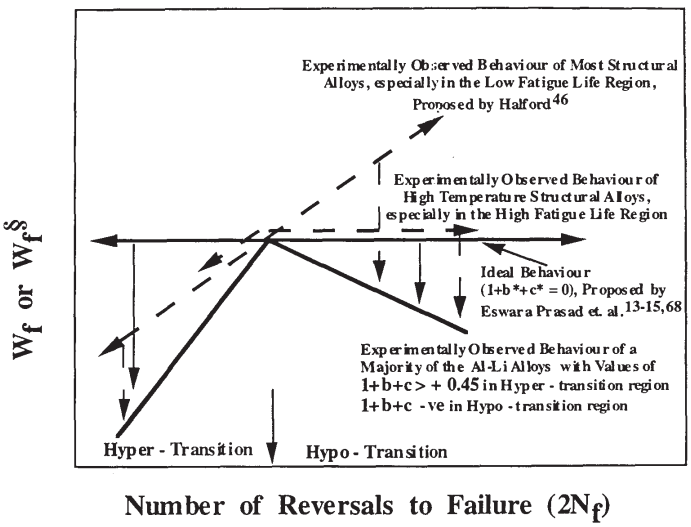

Figure 11. A schematic showing experimental variation of total plastic strain energy till fracture (W_f or $W_f^{\S}$), with number of reversals to failure ($2N_f$) with majority of Al–Li alloys: Experimentally observed behaviour for most structural alloys, proposed by Halford (1971), recently observed experimental behaviour of various high temperature structural alloys (especially in the higher fatigue life region) and the ideal behaviour proposed by Eswara Prasad *et al* (1994, 1996) are also shown.

7. Fracture resistance

Aluminium–lithium alloys suffer from inadequate fracture resistance as compared to the traditionally used structural aluminium alloys. Major alloy developmental activities world-over have been directed to improve the fracture resistance of these alloys. Such an effort has resulted in developing a comprehensive understanding of various metallurgical factors that directly influence the fracture behaviour. Interestingly, these factors also affect tensile ductility and are primarily responsible for limited ductility and inadequate fracture resistance. They are: (i) co-planar deformation and slip localisation (Sanders & Starke 1982; Gregson & Flower 1985; Jata & Starke 1986; Venkateswara Rao & Ritchie 1989a; Eswara Prasad *et al* 1995; Csontos & Starke 2000), (ii) strain localisation at the soft δ'-precipitate free zones (Gysler *et al* 1981; Lin *et al* 1982; Eswara Prasad *et al* 1993a), (iii) presence of coarse, equilibrium precipitates (T_1, δ or T_2 and their variants) and coarse, angular Fe- and Si-bearing inclusions at the low or high angle grain boundaries (Vasudevan *et al* 1986; Vasudevan & Doherty 1987; Suresh *et al* 1987; Lewandowski & Holroyd 1990; Eswara Prasad *et al* 1993a,b), (iv) segregation of alkali elements (Na and K) to grain boundaries and formation of low melting eutectic phases (Wert & Lumsden 1985; Webster 1987) (v) higher hydrogen content causing grain boundary embrittlement (Shin *et al* 1989; Lewandowski & Holroyd 1990) and (vi) fracture along the sub-angle grain boundaries, particularly in unrecrystallised alloys (Starke & Lin 1982; Eswara Prasad *et al* 1993b). Some of the most recent efforts are aimed at ameliorating the impurity effects on grain boundary brittleness with the rare earth additions (Meng *et al* 1998, 2000; Csontos & Starke 2000). These rare earth additions improve intrinsic toughness of these alloys through enhanced grain boundary cohesiveness by reducing the embrittling effects of grain boundary impurities such as Na and K. With such pronounced beneficial effects on fracture toughness as well as isotropy the rare earths have become a regular microalloying addition in Al–Li alloys.

7.1 *Plane-strain fracture toughness* (K_{Ic})

K_{Ic} or the ratio of notch tensile strength to yield strength (NTS/YS) is used as a measure of fracture resistance. Several studies have been conducted to elucidate the effects of various microstructural features such as grain structure, texture, alloy chemistry, aging condition on fracture toughness (Peters & Lutjering 1976; Sanders *et al* 1980; Noble *et al* 1982; Sanders & Starke 1982; Gregson 1984; Gregson & Flower 1985; Jata & Starke 1986; Suresh *et al* 1987; Eswara Prasad & Malakondaiah 1992; Eswara Prasad *et al* 1993a).

In one of the most widely referred works (Gregson 1984; Gregson & Flower 1985), Gregson has shown that fracture resistance of the binary Al–Li alloys can be enhanced significantly by simultaneous additions of Cu and Mg, as compared to the addition of either Cu (which results in T_1 precipitation) or Mg (which enhances the δ' precipitation) independently. As shown in figure 12, simultaneous addition of Cu and Mg improves not only fracture toughness, but also increases the strength level of Al–Li alloys. Such an effect is due to the occurrence of copious amounts of non-coplanar, lenticular shaped, $S(Al_2CuMg)$ precipitates. These precipitates are far more effective in reducing the extent of co-planar slip by effective slip homogenisation as compared to the T_1 precipitates (Gregson 1984). This is because of the non-availability of the potential slip planes in the S phase that are parallel to the matrix slip planes and hence, these S lath precipitates are unlikely to be sheared by dislocations moving through the matrix. The bowing of the dislocations around the S lath precipitates increases local work hardening and reduces slip localisation. However, uniform and dense distribution of S phase is mandatory

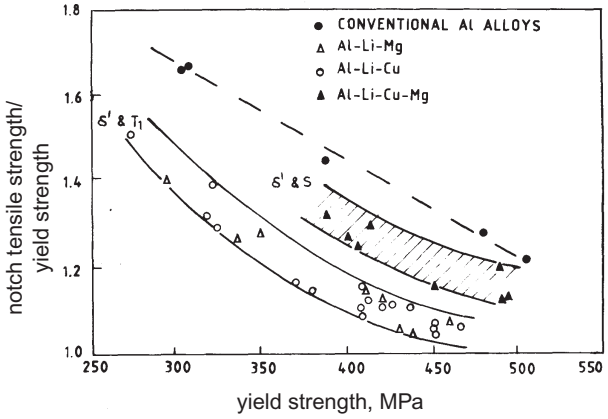

Figure 12. Variation in the ratio of NTS and yield strength (YS) of Al–Li alloys strengthened with δ' and T_1 (in Al–Li with Mg or Cu) and δ' and S (Al–Li with both Mg and Cu). Note the enhancement in the toughness (the ratio of NTS/YS) that occurs from S' precipitates as a result of simultaneous addition of Mg and Cu (from Gregson 1984).

to obtain such beneficial effects. Such an approach is also found to result in higher isotropy in mechanical properties (Gregson 1984; Gregson & Flower 1985).

In another comprehensive study on the combined effects of alloy chemistry and aging condition, Suresh *et al* (1987) have shown that the higher degree of aging up to peak strength aging condition (T3 to T6 temper) results in a decrease in fracture toughness, K_{Ic}. This is the case in three different Al–Li alloys with varied Cu content (see figure 13). However, subsequent aging beyond T6 temper was found to affect fracture toughness differently depending on the Li/Cu ratio in the ternary alloys. In the ternary alloy with low Li/Cu ratio (Li/Cu = 2·2, see figure 13a), the increase in degree of over-aging rapidly increases the fracture toughness. This is due to extensive crack tip deflection and bifurcation, the extent of which is seen to increase with increase in the degree of over-aging. On the other hand, the absence of such

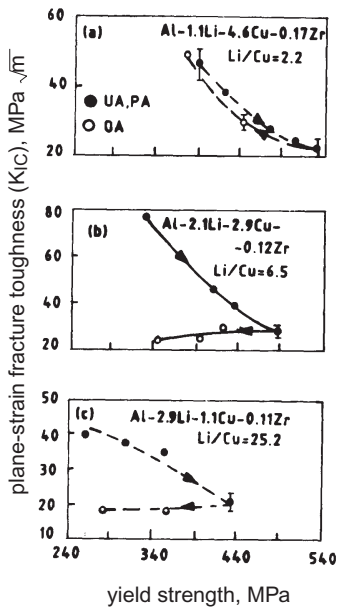

Figure 13. Variation of plane–strain fracture toughness (K_{Ic}) with yield strength in case of Al–Li–Cu alloys with varied Li and Cu contents: **(a)** Li/Cu = 2·2 (ratio of atomic %), **(b)** Li/Cu = 6·5 and (c) Li/Cu = 25·2 (from Suresh *et al* 1987).

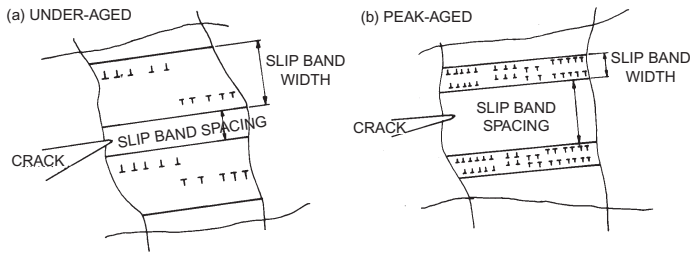

Figure 14. Schematic diagram showing the increase in the ratio of slip band spacing to its width, as occurs from the **(a)** under-aged condition to the peak-aged **(b)** condition, leading to the increasing extent of co-planar slip with ageing.

crack path meandering, the two other ternary Al–Li–Cu alloys with higher Li/Cu ratios (6·5 in figure 13b and 25·2 in figure 13c) exhibit a K_{Ic} value that almost remains constant or even shows a slight decrease with over-aging. In another study, Jata & Starke (1986) have shown that increase in the degree of aging up to peak-aging results in a decrease in fracture toughness, K_{Ic}. These authors have reasoned that such a decrease in fracture resistance is due to the increased extent of planar deformation, which is evidenced in higher slip band spacing to the slip band width ratio (see figure 14).

7.2 *Plane-stress fracture toughness* (K_c)

Plane-stress conditions occur in alloy sheets. Thickness dependent K_c offers a measure of fracture toughness, while K_R–Δa (R-curve) behaviour depicts overall fracture resistance in sheet materials (Broek 1986). Al–Li alloys typically exhibit flat R-curves. This is especially so when the crack extension is along the rolling direction (Kamat & Eswara Prasad 1990; Eswara Prasad *et al* 1993b). Apart from this, numerous microstructural modifications are adopted to enhance the R-curve resistance of Al–Li alloys. These microstructural modifications invariably employed recrystallised grain structure (to principally achieve a desired degree of isotropy as well as enhanced K_c) and suitable processing schedules to enhance the texture influenced crack path tortuosity (McDarmaid & Peel 1989; Eswara Prasad *et al* 1993b).

In a comprehensive analysis conducted on crack deflection and branching and their effects on the R-curve behaviour in Al–Li alloys, Eswara Prasad *et al* (1993b) have derived a relationship. This relation brings out contributions to K_R of the following: (a) crack deflection, (b) symmetrical crack branching, (c) asymmetrical crack branching and (d) combined conditions of crack deflection and branching:

$$(K_R)_{D,Br} = (K_R)_{UD,UBr}\ \mathrm{Sec}^{1/2}\Theta Q\{1 + \Sigma[F'(2\alpha, b/a) - 1]_m\}, \tag{3}$$

where UD and D refer to the undeflected and deflected conditions respectively; similarly, UBr and Br refer to the unbranched and branched conditions. Θ is the deflection angle and α is the half of the branch including angle, a and b are lengths of the branch ligaments (for symmetrical branching $a = b$). 'm' is the number of branching events. 'F' is an analytical (in case of the finite or infinitely small branched cracks that are symmetrical) or numerical (in case of asymmetrically branched cracks) function of α and a and b. Contribution to K_R from the enhanced crack-tip plasticity is retained in $(K_R)_{UD,UBr}$ variation with the crack extension, Δa. Such a treatment of fracture resistance data enables quantitative determination of the

Table 4. Plane-stress fracture toughness (K_c) data of a few selected Al–Li alloys.

Alloy & temper designations	Dominant microstructural features	Test direction	0·2% Yield strength (MPa)	K_c (MPavm)	Ref.
AA 8090–T81	Fine δ' and unrecrystallised grain structure	L/L–T	436	75	Grimes *et al* (1987)
	Fine δ' and recrystallised grain structure	L/L–T	360	118	
AA 2090–T8X				120	
AA 8090–T81 (1·6 mm thick, 400 mm wide panel)	Fine δ' and equiaxed, recrystallised grain structure	L/L–T	323	143	Miller *et al* (1987)
	Fine δ' and laminar, recrystallised grain structure	L/L–T	317	98	
AA 8090–T81 (1·6 mm thick, 250 mm wide panel)	Fine δ' and equiaxed, recrystallised grain structure	L/L–T LT/T–L	335 306	114 95	McDarmaid & Peel (1989)
AA 2024–T3 (Al clad – 1·6 mm thick and 250 mm wide panel)		L/L–T LT/T–L	314 286	118 114	
AA 2090–T83	Coarse δ' and recrystallised grain structure	L/L–T	505	43	Venkateswara Rao *et al* (1990)
AA 8090–T6 (1–3 mm thick, 100 mm wide) panels)	Coarse δ' and unrecrystallised grain structure	L/L–T LT/T–L	456 426	46–54 44–51	Kamat & Eswara Prasad (1990)
AA 2090–T6 (4·5 mm thick, 100 mm wide) panels)	Coarse δ' and unrecrystallised grain structure	L/L–T LT/T–L	456 461	74 46	Eswara Prasad *et al* (1993b)

individual contributions of various microstructural modifications to the plane-stress fracture resistance of alloy sheets in general and those for the Al–Li alloy sheets, in particular (Eswara Prasad *et al* 1995).

Fracture resistance data of several Al–Li alloys broadly show that these alloys have significantly lower plane-stress fracture resistance (K_c) as compared to the traditionally used aluminium alloy 2024 (table 4). However, a closer examination of the data in table 4 indicates that the recently developed commercial alloys with fine recrystallised grain structure and those containing fine δ' precipitates (in underaged or near-peakaged condition, specifi-

cally the AA 8091 in the T81 temper) have possessed a strength (σ_{ys}) and fracture toughness (K_c) combination comparable to that of the AA 2024 alloy. Further, the study by Grimes *et al* (1987) suggests that the use of recrystallised grain structure results in significantly enhanced fracture resistance (nearly 40% higher K_c; see data in table 4).

7.3 *Anisotropy in the fracture resistance*

Thick products constitute larger portions of Al alloy parts in the over-all metallic content of the materials that are used in a modern aircraft. The principal difficulty of producing these thick products has been to develop desired property levels with the desired level of isotropy. Such a task has been a most challenging aspect of the development of these alloys till date as will be shown in this section.

Co-planar slip is the principal contributing factor to directionality as well as in limiting fracture toughness of Al–Li alloys. This is because of directionality in the shearing nature of the strengthening precipitates, δ' and T_1, apart from the directionality of the weak low and high angle grain boundaries. Eswara Prasad and co-workers (1993a and 1994) have shown that in-plane anisotropy in fracture toughness under both static and dynamic loading conditions is due to the combined effects of crystallographic texture and grain fibering, distribution of the coarser and angular equilibrium precipitates (in their case T_2) that act as sites for void nucleation, growth and coalescence.

In another comprehensive study, Venkateswara Rao & Ritchie (1989) have evaluated and shown that most of Al–Li alloys exhibit considerable through-thickness anisotropy. The pronounced disparity in the K_{Ic} values of Al–Li alloy plates in the rolling plane (L–T or T–L orientation) as compared to the thickness direction (S–L or S–T) is attributed to crystallographic texture and the nature and extent of delamination fracture. The extent of disparity is evident from the data shown in figure 15, where the fracture toughness data of several Al–Li alloys are given along with those for the traditionally used structural Al alloys in the two test direc-

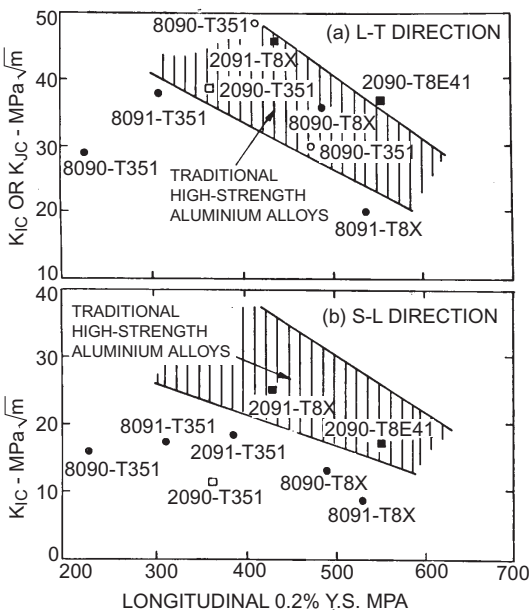

Figure 15. Fracture resistance of Al–Li alloys in L–T (notch being oriented perpendicular to the rolling direction) and S–L (notch being oriented in the through-thickness direction) notch orientations (from Venkateswara Rao & Ritchie 1989).

tions – one in the rolling plane, L–T and the other in the thickness plane, S–L. Another study conducted to reduce the through-thickness anisotropy in fracture resistance, Lynch (1991) has shown that double aging treatment significantly enhanced fracture toughness in the through-thickness direction, thereby reducing the disparity between the K_{Ic} values of principal crack orientations. The double aging treatment involves reaging after initial artificial aging at significantly higher temperatures of 200–210°C (with rapid heating to the reaging temperatures) for shorter durations of up to 300 s. The beneficial effect is attributed to the extent of Li segregation to the high angle grain boundaries which makes these boundaries stronger.

7.4 *Fracture resistance under shear loading*

Studies on quasi-static fracture resistance of most of the structural alloys have been evaluated under mode-I or tensile loading conditions. However, flaws in engineering structures seldom experience pure mode-I loading and hence, it is essential to evaluate fracture resistance of promising structural materials under the other modes of failure, such as mode-II or in-plane shear or mode-III or anti-plane shear or even combinations of these three general modes of loading. Eswara Prasad and co-workers (Eswara Prasad *et al* 1994; Eswara Prasad & Kamat 1995) have shown that AA8090 Al–Li alloy in the underaged condition possesses a low value of fracture toughness in mode-II or in-plane shear loading condition and a high value of fracture toughness in mode-I or tensile loading with an intermediate value of fracture toughness in mode-III or anti-plane shear. On the other hand, the trend is opposite when the alloys are aged to peak strength. The fracture resistance under mode-III loading becomes the highest and the mode-I toughness the lowest, while the mode-II fracture resistance is intermediate (see data in table 5). The observed behaviour has been explained in terms of the extent and the ease with which shearing of the strengthening precipitates occurs. The shearing of the strengthening precipitates (especially the spherical δ') becomes progressively difficult with precipitate coarsening during aging and hence, the alloys exhibit lower resistance to fracture under shear loading when they are in an underaged condition. This finding has acquired importance because the material developers have recognised underaging as one of the means to enhance mode-I or tensile fracture toughness. Such a stratagem should be viewed with caution in light of these findings. This means that there exists an optimum window of strength and fracture resistance (a minimum value among the three general modes of loading) for each of the alloys and product forms, which needs to be determined for the optimisation of the alloy composition or aging or any other thermomechanical condition. These findings clearly indicate that any attempt to improve the mode-I fracture resistance even at the cost of some strength should not be blindly resorted to because of a possible decrease in fracture resistance in the other two modes of loading or under mixed-mode loading conditions.

8. Fatigue crack growth resistance

Most of the studies reported till date on the fatigue crack growth (FCG) resistance of Al–Li alloys, including those under spectrum loading conditions, have unequivocally shown that these alloys possess a significantly higher FCG resistance as compared to the traditionally used aluminium alloys (Coyne *et al* 1981; Harris *et al* 1983; Vasudevan *et al* 1984; Suresh & Ritchie 1984; Jata & Starke 1986; Venkateswara Rao & Ritchie 1988; Wanhill *et al* 1991; Sunder 1991; Wanhill 1994; McEvily & Ritchie 1998; McMaster *et al* 1998; Cui *et al* 2000; Chen & Cheturvedi 2000). This behaviour was originally attributed to the higher elastic modulus properties of these alloys and consequently to the less accumulated crack-tip damage due

Table 5. Fracture resistance of AA 8090 alloy plates under general modes of loading (data from Eswara Prasad *et al* 1994).

Description	AA 8090 in underage ($T3$) temper condition		AA 8090 in peakage (T8E51) temper condition	
Stress / Notch orientation	L / L–T	LT / T–L	L / L–T	LT / T–L
0·2% Yield strength (MPa)	410	380	485	467
Ultimate tensile strength (MPa)	470	470	555	534
Shear modulus (μ) (GPa)	30·1	30·1	30·5	30·5
Mode-I fracture toughness (K_{Ic} or K_{Jc}) (MPa vm)	49	48	28	16
Mode-II fracture toughness (K_{IIQ}) (MPa vm)	32	Unstable crack extension	32	36
Mode-III fracture toughness: K_{IIIQ}, derived from J_{IIIQ} with notches of root radius of 80 μm (MPa vm)	41	38	54	46
Tearing modulus $(T_R)_{III}$	14·1	4·2	19	10·4
Slope of the J_{III}–Δa curve, dJ_{III}/da (MJ/m^3) (another measure of fracture resistance)	23	6·3	42	21
Mode-III, exclusive fracture toughness, $(J_{III})_{Exc.}$, kJ/m^2 (measure of fracture resistance at a crack extension of 1·5 mm)	64	34	124	68

to pronounced slip reversibility (Coyne *et al* 1981; Harris *et al* 1983). Higher slip reversibility under fatigue loading conditions is a direct result of slip co-planarity, which provides a beneficial effect in case of the FCG behaviour. Studies by Venkateswara Rao & co-workers (Venkateswara Rao & Ritchie 1989, 1990, 1992; Venkateswara Rao *et al* 1988a, 1991) have clearly shown that the higher FCG resistance in Al–Li alloys is indeed due to the pronounced crack tip shielding induced in part from the strong co-planarity of the slip; but primarily by the predominant crack closure levels due to the crack path deflection and bifurcation, apart from the plasticity-induced and asperity-induced wedging crack closure. These factors enhance closure and result in superior fatigue crack growth resistance in Al–Li alloys (see figure 16).

The pronounced crack path meandering (deflection with or without branching and bifurcation) is due to the texture-controlled plasticity that occurs due to the shearing of δ' precipitates and the resulting shear band fracture along the close packed {111} crystallographic planes, which in turn results in crystallographic faceted fracture and the related asperity-induced wedging crack closure (Suresh *et al* 1984; Vasudevan *et al* 1984; Venkateswara Rao & Ritchie 1988; Venkateswara Rao *et al* 1991 and Rading & Berry 1996; Guvenilier & Stock 1998; Chen & Chaturvedi 2000). Based on such micromechanism(s), Venkateswara Rao *et al* (1991) have shown that the higher degree of crack closure occurs in plate products as compared to the sheet product. The data in figure17a show that the FCG resistance of the plate product is sig-

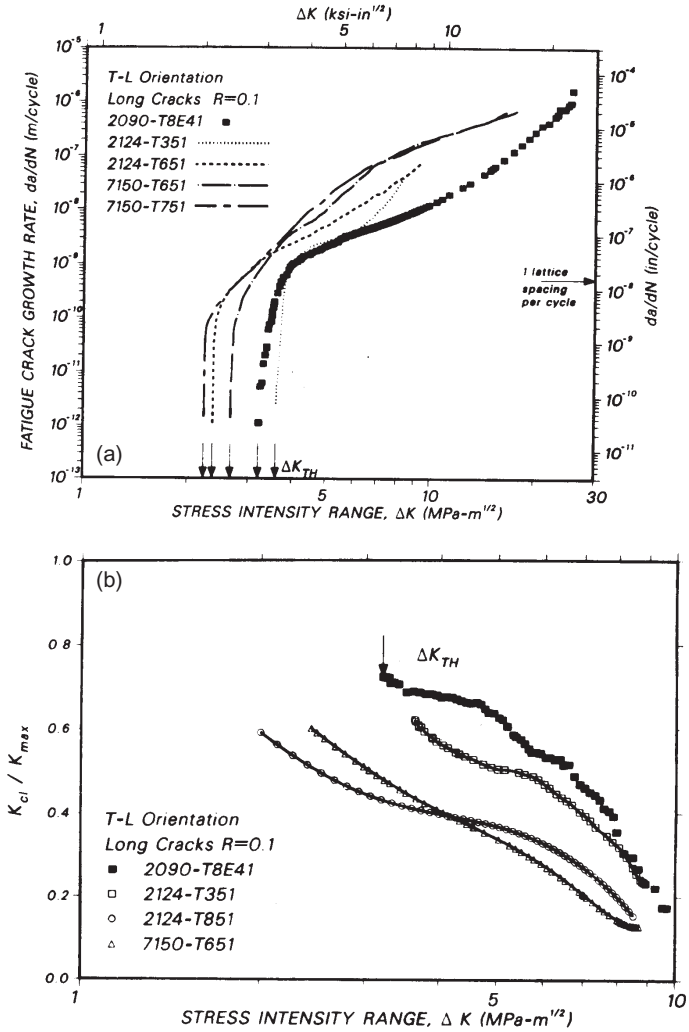

Figure 16. Fatigue crack growth behaviour of several Al alloys as compared to the Al–Li alloy AA2090–T8E41: **(a)** variation of crack growth rates and **(b)** extent of crack closure ($K_{cl}/K_{\max}$) with ΔK. The AA 2090 alloy exhibits superior FCG resistance due to higher extent of crack closure (Venkateswara Rao *et al* 1991).

nificantly higher (particularly at the lower values of the stress intensity factor range) as compared to that of the sheet product. Figure 17b shows the corresponding fatigue crack path and figure 18 the related morphologies. The higher crack closure means higher values of K_{cl} (the stress intensity factor till which the crack is dormant) for a particular $K_{\max}$ and R-ratio. This is reflected in higher values of $K_{cl}/K_{\max}$ in figure 17b for the plate as compared to the sheet.

Subsequent studies on high purity quaternary Al–Li–Cu–Mg alloys with varied content of Cu and Li have shown that the superior FCG resistance in these alloys is also due to the varied extent of precipitate shearing and the resultant slip planarity (Vasudevan & Suresh 1985; Jata & Starke 1986; Petit *et al* 1986; Chen & Li 1989; Tintillier *et al* 1989). The studies on δ' and T_1 precipitation and reversion indicate that the T_1 precipitates inhibit co-planar slip to a

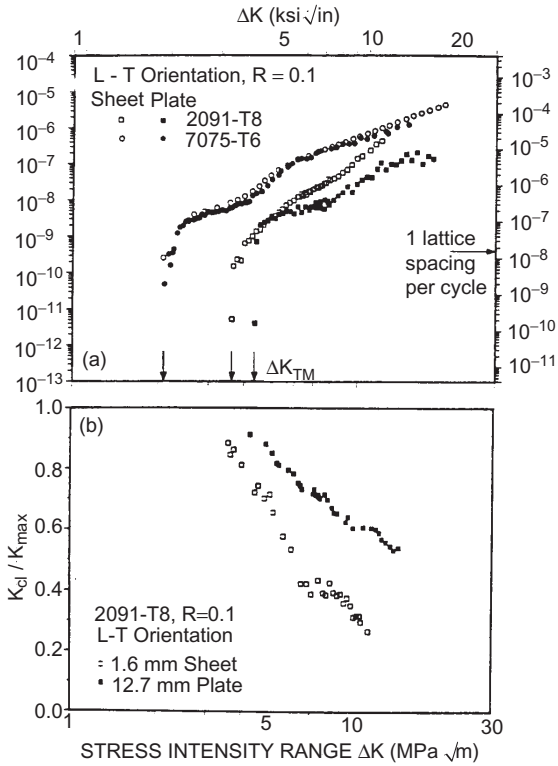

Figure 17. **(a)** Fatigue crack growth rates and **(b)** normalized crack closure levels in AA 2090–T8 sheet and plate, in the LT orientation at $R = 0{\cdot}1$, as a function of nominal stress intensity range, (ΔK). Growth rate data are compared with corresponding results on 7075-T6 alloys (from Venkateswara Rao *et al* 1991).

certain extent, when the Li content is low. The resultant crack closure levels are moderate. On the other hand, Petit *et al* have shown that when Li content is high, the effectiveness of T_1 precipitates to reduce co-planar slip is negligible. Hence, the alloy shows still higher fatigue crack growth resistance.

The enhanced FCG resistance in Al–Li alloys is evident only when the cracks assume a finite size, i.e., when they are mechanically and/or microscopically long cracks (Venkateswara Rao *et al* 1988). Studies conducted on this aspect, clearly indicated that due to the pronounced crack tip shielding and the resultant higher levels of crack closure, Al–Li alloys exhibit superior FCG resistance only in the long crack growth regime of the fatigue damage domain and thus, compare favourably when compared with the FCG resistance of traditional aluminium alloys such as AA 2124 and AA 7150. On the other hand, at equivalent stress intensity factor ranges, the growth rates of the smaller cracks (both mechanically and microstructurally smaller cracks where a limited wake zone inhibits the crack tip shielding to a lesser extent) are typically three orders of magnitude higher at the near-threshold levels. Such behaviour was found to be the case for Al–Li alloys when they are tested for in-plane (L–T and T–L) as well as through-thickness (T–S) orientations.

9. Current status of and future directions for alloy development

Although the potential of Al–Li based alloys on account of weight savings has been acknowledged, the promise of these alloys in a wide range of aeronautical systems has not materialised

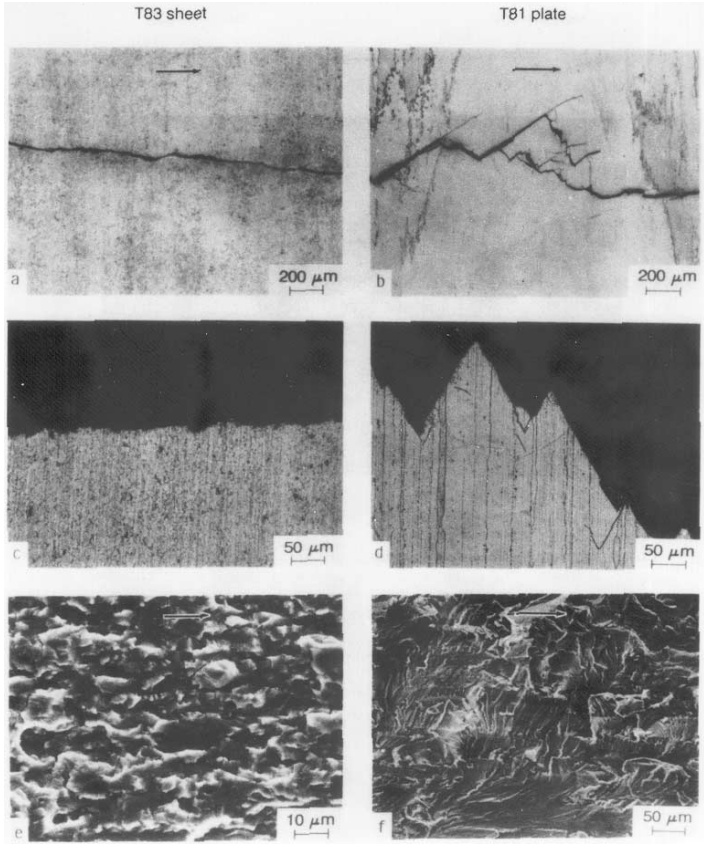

Figure 18. Comparison of fatigue crack path and fracture surface morphologies in AA 2090 alloy processed as T83 sheet and T81 plate, showing **(a, b)** crack paths along the crack growth direction, **(c, d)** crack profiles across the specimen thickness and **(e, f)** fracture surfaces. Arrows indicate the general direction of crack growth (from Venkateswara Rao *et al* 1991).

yet. Difficulties in melt processing, necessitate segregating scrap from other alloys. This aspect, as also high cost of the raw materials, are the important hindrances to wide scale commercial exploitation.

Efforts in Al–Li alloy development have been extensive and multidirectional. Some of the directions pursued are:

(i) Modifications in microstructural features and texture characteristics, as obtainable by a proper selection of composition and processing schedules. These should improve the property levels substantially with reasonable isotropy and adequate damage tolerance in these alloys. In this context, the beneficial effect of slip homogenising phases such as S and S' has been well established.

(ii) Optimum levels of degree of recrystallisation and finer grain sizes within the allowable reductions in the section sizes of various products should be obtained.

(iii) Novel alloy development efforts in the direction of major and minor alloying additions of rare earth (especially Ce), Sc, Be, TiB and Ag are to be pursued to a logical conclusion.

(iv) The content of coarse equilibrium phases such as δ, T_2; angular particles of Fe and Si; and finally the content of alkali elements such as Na and K and dissolved hydrogen should be kept to a minimum.
(v) Currently, in a major R & D programme on nano-crystalline bulk materials, Inoue group in Japan have obtained strength levels in excess of 1000 MPa (Masumoto & Inoue 1998; Inoue *et al* 2001). This approach could provide another avenue for developing improved Al–Li alloys.
(vi) Finally, the major alloy modifications and changes in processing, thermal and thermo-mechanical treatments should be evaluated comprehensively so that optimum property combinations could be arrived at more systematically.

The aforementioned are applicable to any product form, such as plate or sheet or forging block, or an extruded rod. However, it should be noted that different product forms, depending on their application and principal loading directions, require different combinations of properties - strength, toughness and isotropy. For example, high strength, enhanced low cycle fatigue resistance, high fatigue crack growth resistance and adequate degree of fracture resistance and isotropy are required for thick plate products; while higher degree of isotropy and enhanced fracture resistance even at the cost of strength are required for thin sections of sheets and other products. Hence, optimised alloy specifications (see table 6) in terms of composi-

Table 6. Comparison of the fatigue and fracture properties of various optimised Al–Li alloy products as compared to the conventional Al alloys (compiled from Wanhill 1994).

Strength level	Product form	HCF & NFS	FCGR		Strength–fracture toughness combinations
			Short cracks	Long cracks	
High strength	Sheet (2090-T83)	+ve / =	=	+ve	−ve
	Plate (8090-T851) & extrusions (2090-T86)	+ve / =	=	+ve	+ve at CT and = at RT & −ve in plate directions of S–L/S–T
Medium strength	Sheet (8090-T92)	+ve / =	+ve	+ve	−ve
	Extrusions (8090-T8511)	+ve / =		+ve	+ve at CT and = at RT
Low strength & damage tolerance	Sheet (2091-T84 & 8090-T81)	+ve / = +ve	= =	+ve / = +ve / =	−ve +ve at CT & RT
	Plate (8090-T8171 & 8090-T86)				

Nomenclature: HCF – high cycle fatigue; NFS – notch fatigue strength; FCGR – fatigue crack growth resistance; CT – cryogenic temperatures; RT – room temperature; +ve – superior; −ve – inferior; = – equal or equivalent.

tion and temper conditions or thermomechanical treatments are different for different alloy products of varied strength level.

Finally, a new approach based on a highly refined ingot grain size, resulted in fine, but unrecrystallised, grain structure. This approach employs hermomechanical processing that promotes recrystallisation in the early steps of rolling, followed by processing under non-recrystallising conditions yields a microstructure in which the original grain boundaries are 'freed' from as-cast segregation products and later developed into a fine unrecrystallised structure. Such a microstructure may be optimum in realising an acceptable combination of strength, toughness and isotropy.

10. Conclusions

(1) Al–Li alloys are prime candidate materials to replace traditionally used Al alloys. Despite their numerous property advantages, low tensile ductility and inadequate fracture toughness, especially in the through thickness-directions, militate against their acceptability.
(2) Extensive co-planar slip, sensitivity towards the presence of even low contents of alkali metals, hydrogen and some of the impurities are key factors responsible for the property limitations.
(3) It is now possible to obtain alloys in different thermal and thermo-mechanical conditions that are suitable for different product forms. However, further efforts are needed to suitably modify the microstructure and crystallographic texture in order to improve isotropic mechanical behaviour and enhance damage tolerance of these alloys.
(4) Understanding of mechanical behaviour and the related micromechanisms in these alloys has helped to a significant extent the use of Al–Li alloys for certain structural applications.

Financial assistance from the Defence Research and Development Organisation is acknowledged with thanks. The authors thank colleagues at Defence Metallurgical Research Lab who have contributed to some of the studies reported in this review article. One of the authors (NEP) gratefully acknowledges the support of Alexander von Humboldt Foundation, Bonn, Germany, through a special grant (No. V-8151/20034-INI/1053979). Finally, the authors express profound gratitude to Dr D Banerjee for his encouragement.

References

Adam C M 1981 Overview of DC casting. In *Aluminium–lithium alloys; Proc. First Int. Conf. Aluminium–Lithium Alloys* (eds) T H Sanders, E A Starke (Warrendale, PA: AIME) pp 37–48

Balabhaskaran K, Satya Prasad K, Vijaya Singh, Gokhale A A 1999 (unpublished work)

Balmuth E S 1994 The status of Al–Li alloys, in aluminium alloys: Their physical and mechanical properties. In *Proc. 4th Int. Conf. Aluminium Alloys* (eds) T H Sanders, E A Starke (Atlanta: Georgia Inst. Technol.) pp 82–89

Balmuth E S, Chellman D J 1987 Alloy design for overcoming the limitations of Al–Li alloy plate. *J. Phys. (Paris)* 48: c3.293–c3.299

Banerjee S, Ayra A, Das G P 1997 Foundation of an ordered intermetallic phase from a disordered solid solution - A study using first principles calculation in Al–Li alloys. *Acta Metall.* 45: 601–609

Bavarian B, Becker J, Parikh S N, Zamanzadeh M 1989 Localised corrosion of 2090 and 2091 Al–Li alloys. In *Proc. 5th Int. Conf. Aluminium–Lithium Alloys* (eds) T H Sanders, E A Starke (Birmingham, UK: Mater. Components Eng. Publ.) vol. 2, pp 1227–1236

Birch M E J, Cowell A J 1987 Titanium–carbon–aluminium: A novel grain refiner for aluminium–lithium alloys. *J. Phys. (Paris)* 48: c3.103–c3.108

Bird R K, Discus D L, Fridyander I N, Sandler V S 2000 Al–Li alloy 1441 for fuselage applications. *Mater. Sci. Forum* 331–337: 907–912

Broek D 1986 *Elementary engineering fracture mechanics* (Dordrecht: Martinus Nijhoff)

Chakravorty C R 1988 *Studies on the characteristics of cast binary aluminium–lithium alloys*. Doctoral thesis, Indian Institute of Technology, Kharagpur

Chen C Q, Li H X 1989 Crack path profiles of Al–Li single crystals under monotonic and cyclic loading. In *Aluminium–lithium alloys* (eds) T H Sanders, E A Starke (Birmingham, UK: Mater. Components Eng. Publ.) vol. 2, pp 973–981

Chen D L, Chaturvedi M C 2000 Near-threshold fatigue crack growth behaviour of 2195 aluminium–lithium alloy – prediction of crack propagation direction and influence of stress ratio. *Metall. Mater. Trans.* A31: 1531–1541

Coyne E J, Sanders T H, Starke E A 1981 The effect of microstructure and moisture on the low cycle fatigue and fatigue crack propagation of two Al–Li–X alloys. In *Aluminium–lithium alloys* (eds) T H Sanders, E A Starke (Warrendale, PA: Metall. Soc. AIME) pp 293–305

Clarke E R, Gillespie P, Page F M 1986 Heat treatments of Li/Al alloys in salt baths. In *Aluminium–lithium alloys* (eds) C Backer, P J Gregson, S J Harris, C J Peel (London: Ins. Metals) vol. 3, pp 159–163

Csontos A A, Starke E A 2000 The effect of processing and microstructure development on the slip and fracture behaviour of the 2·1 wt.% Li AF/C-489 and 1·8 wt. % Li AF/C-458 Al–Li–Cu–X alloys. *Metall. Mater. Trans.* A31: 1965–1976

Cui J, Fu Y, Li N, Sun J, He J, Dai Y 2000 Study on fatigue crack propagation and extrinsic toughening of an Al–Li alloy. *Mater. Sci. Eng.* A281: 126–131

Dhers J, Driver J, Foundeux A 1986 Cyclic deformation of binary Al–Li alloys. In *Aluminium–lithium alloys* (eds) C Baker, P J Gregson, S J Harris, C J Peel (London: Inst. Met.) vol. 3, pp 233–238

Edwards M R, Stoneham V E 1987 The fusion welding of Al–Li–Cu–Mg 8090 alloy. In *J. Phys. (Paris)* 48: c3.293–c3.299

Ekvall J C, Rhodes J E, Wald G G 1982 *Methodology for evaluating weight savings from basic material properties* ASTM STP 761 (Philadelphia, PA: Am. Soc. Testing Mater.) pp 328–341

Engler O, Sachot E, Ehrstrom J C, Reeves A, Shahani R 1996 Recrystallisation and texture in hot deformed aluminium alloy 7010 thick plates. *Mater. Sci. Technol.* 12: 717–729

Eswara Prasad N 1993 *In-plane anisotropy in the fatigue and fracture properties of quaternary Al–Li–Cu–Mg alloys*. Doctoral thesis, Banaras Hindu University, Varanasi

Eswara Prasad N, Kamat S V 1995 Fracture behaviour of quaternary Al–Li–Cu–Mg alloys under mixed-mode I/III loading. *Metall. Mater. Trans.* A26: 1823–1833

Eswara Prasad N, Malakondaiah G 1992 Anisotropy in the mechanical properties of quaternary Al–Li–Cu–Mg alloys. *Bull. Mater. Sci.* 15: 297–310

Eswara Prasad N, Rama Rao P 2000 Low cycle fatigue resistance in Al–Li alloys. *Mater. Sci. Technol.* 16: 408–426

Eswara Prasad N, Malakondaiah G, Raju K N, Rama Rao P 1989 Low cycle fatigue behaviour of an Al–Li alloy. In *Advances in fracture research* (eds) K Salama, K Ravi-Chander, D M R Taplin, P Rama Rao (New York, PA: Pergamon) pp 1103–1112

Eswara Prasad N, Satya Prasad K, Malakondaiah G, Banerjee D, Gokhale A A, Sundararajan G, Chakravorty C R 1991 Microstructure and mechanical properties of 1420 Al–Mg–Li alloy sheet product. DMRL Tech. Report No. 91128, Defence Metallurgical Research Laboratory, Hyderabad

Eswara Prasad N, Malakondaiah G, Rama Rao P 1992 Strength differential in Al–Li alloy 8090. *Mater. Sci. Eng.* A150: 221–229

Eswara Prasad N, Kamat S V, Malakondaiah G 1993a Effect of crack deflection and branching on *R*-curve behaviour of an Al–Li alloy 2090 sheet. *Int. J. Fracture* 61: 55–69

Eswara Prasad N, Kamat S V, Prasad K S, Malakondaiah G, Kutumbarao V V 1993b In-plane anisotropy in fracture toughness of an Al–Li 8090 plate. *Eng. Fracture Mech.* 46: 209–223

Eswara Prasad N, Paradkar A G, Malakondaiah G, Kutumbarao V V 1994a An analysis based on plastic strain energy for bilinearity in Coffin–Manson plots in an Al–Li alloy. *Scr. Metall. Mater.* 30: 1497–1502

Eswara Prasad N, Kamat S V, Prasad K S, Malakondaiah G, Kutumbarao V V 1994b Fracture toughness of quaternary Al–Li–Cu–Mg alloy under mode I, mode II and mode III loading conditions. *Metall. Mater. Trans.* A25: 2439–2452

Eswara Prasad N, Prasad K S, Kamat S V, Malakondaiah G 1995 Influence of microstructural features on the fracture resistance of aluminium–lithium alloy sheets. *Eng. Fracture Mech.* 51: 87–96

Eswara Prasad N, Malakondaiah G, Kutumbarao V V, Rama Rao P 1996 In-plane anisotropy in low cycle fatigue properties of and bilinearity in Coffin–Manson plots for quaternary Al–Li–Cu–Mg 8090 alloy plate. *Mater. Sci. Technol.* 12: 563–577

Eswara Prasad N, Malakondaiah G, Kutumbarao V V 1997 On the micromechanisms responsible for bilinearity in fatigue power-law relationships in aluminium–lithium alloys. *Scr. Mater.* 37: 581–587

Fragomemi J M, Hillberry B M, Sanders T H 1989 An investigation of the d' particle strengthening mechanisms and microstructure for an Al–Li–Zr alloy. *Aluminium–lithium alloys* (eds) T H Sanders, E A Starke (Birmingham: Mater. Components Eng. Publ.) vol. 2, pp 837–848

Flower H M, Gregson P J 1987 Critical assessment: Solid state phase transformations in aluminium alloys containing lithium. *Mater. Sci. Technol.* 3: 81–90

Fridlyander I N, Shiryaeva N V, Ambortsumyan S M, Gorokhova T A, Gadidullin R M, Sidorov N G, Sorokin N A, Kuznetsov A N 1967 Aluminium based alloy. *British Patent* No. 1, 172, 736

Fridlyander I N 1989 Aluminium–lithium weldable alloy 1420. In *Aluminium–lithium alloys* (eds) T H Sanders, E A Starke (Birmingham: Mater. Component Eng. Publ.) vol. 3, pp 1359–1364

Fridlyander J N, Kolobnev N I, Khokhlatova L B, Lovchelt E, Winkler P J, Pfannenmuller T 1998 Properties of New Al–Li–Mg Alloy. In *Aluminium alloys: Their physical and mechanical properties* (eds) T Sata, T Kumai, Y Murakami (Tokyo: Japan Inst. Metals) vol. 2, pp 2055–2060

Fridlyander J N, Kolobnev N I, Khokhlatova L B, Tarasenko L V, Zhegina I P 1998b Study of the structure and properties of 1420 alloy modifications for sheets. In *Aluminium alloys: Their physical and mechanical properties* (eds) T Sata, T Kumai, Y Murakami (Tokyo: Japan Inst. Metals) vol. 3, pp 2055–2060

Gokhale A A, Ramachandran T R 1990 Development of aluminium–lithium alloys. *Indian J. Technol.* 28: 235–246

Gokhale A A, Satya Prasad K, Vikas Kumar, Chakravorty C R, Leschiner L N, Mozharovsky S M, Fridlyander I N 1994a An aluminium–lithium alloy with improved in-plane anisotropy. In *Aluminium alloys: Their physical and mechanical properties* (eds) T H Sanders, E A Starke (Georgia, Atlanta: Georgia Inst. Technology) vol. 2, pp 428–435

Gokhale A A, Vijaya Singh, Eswara Prasad N, Chakravorty C R, Prasad Y V R K 1994b Processing maps for Al–Li alloys. In *Aluminium alloys: Their physical and mechanical properties* (eds) T H Sanders, E A Starke (Georgia, Atlanta: Georgia Inst. of Technol.) pp 242-249

Gokhale A A, Singh V, Prasad K S, Eswara Prasad N, Chakravorty C R 1998 Development of high specific strength aluminium alloys for aerospace structural applications. *Proc. Int. Conf. Aluminium, INCAL '98* (eds) D H Sastry, S Subramanian, K S S Murty, K P Abraham (Bangalore, India: Aluminium Assoc. India) vol. 2, pp 101–106

Gokhale A A, Singh V, Varma V K 2000 (unpublished work)

Gregson P J 1984 Doctoral thesis, University of London, London

Gregson P J, Flower H M 1985 Microstructural control of toughness in aluminium–lithium alloys. *Acta Metall.* 33: 527–537

Gregson P J, Flower H M, Tete C N J, Mukhopadhyay A K 1986 Role of vacancies in precipitation of δ' and S phases in Al–Li–Cu–Mg alloys. *Mater. Sci. Technol.* 2: 349–353

Grimes R 1990 Aluminium–lithium based alloys. *Encyclopedia materials science engineering* (eds) R W Cahn (New York: Pergamon) vol. 2, pp 667–678

Grimes R, Davis T, Saxty H J, Fearon J E 1987 Progress to aluminium–lithium semi-fabricated products. *J. Phys. (Paris)* 48: c3.11–c3.24

Guvenilir A, Stock S R 1998 High resolution computed topography and implications for fatigue crack closure modelling. *Fatigue Fracture Eng. Mater. Struct.* 21: 439–450

Gysler A, Crookes R, Starke E A 1981 A comparison of microstructure and tensile properties of P/M and I/M Al–Li–X alloys. In *Aluminium–lithium alloys* (eds) T H Sanders, E A Starke (Warrendale, PA: Metall. Soc. AIME) pp 263–291

Hales S J, Hafley R A 1998 Texture and anisotropy in Al–Li alloy 2095 plate and near-net-shape extrusions. *Mater. Sci. Eng.* A257: 153–164

Halford G R 1966 The energy required for fatigue. *J. Mater.* 1: 3–29

Harris S J, Noble B, Dinsdale K 1984 Effect of composition and heat treatment on strength and fracture characteristics of Al–Li–Mg alloys. In *Aluminium–lithium alloys* (eds) T H Sanders, E A Starke (Warrendale, PA: Metall. Soc. AIME) pp 219–233

Heikkenen H C, Lin F S, Starke E A 1981 The low cycle fatigue behaviour of high strength 7XXX type aluminium alloys in the T7351 condition. *Mater. Sci. Eng.* 51: 17–23

Inoue A, Kawamura Y, Kimura H M, Mano H 2001 Nanocrystalline Al-based bulk alloys with high strength above 1000 MPa. *Mater. Sci. Forum* 360–362: 129–136

Jata K V, Starke E A 1986 Fatigue crack growth and fracture toughness behaviour of an Al–Li–Cu alloy. *Metall. Trans.* A17: 1011–1026

Jata K V, Hopkins A K, Rioja R J 1996 The anisotropy and texture of Al–Li alloys. *Mater. Sci. Forum* 217–222: 647–652

Jata K V, Panchandeeswaran S, Vasudevan A K 1998 Evolution of texture, microstructure and mechanical property anisotropy in an Al–Li–Cu alloy. *Mater. Sci. Eng.* A257: 37–46

Jha S C, Sanders T H, Dayananda M A 1987 Grain boundary precipitate free zones in Al–Li alloys. *Acta Metall.* 35: 473–482

Kamat S V, Eswara Prasad N 1990 Mixed-mode analysis of crack deflection and its influence on R-curve behaviour of aluminium–lithium 8090 alloy sheets. *Scr. Metall. Mater.* 24: 1907–1912

Kamat S V, Eswara Prasad N, Malakondaiah G 1991 Comparison of mode I and mode II fracture toughness of an 8090 Al–Li alloy. *Mater. Sci. Eng.* A149: L1–L3

Khireddine D, Rahouadj R, Clavel M 1989 The influence of δ' and S' precipitation on low cycle fatigue behaviour of an aluminium alloy. *Acta Metall.* 37: 191–201

Kim N J, Bye R L, Das S K 1987 Recent developments in rapidly solidified aluminium–lithium alloys. In *Aluminium–lithium alloys: Design, development and applications update* (eds) R J Kar, S P Agrawal, W E Quist (Metals Park, OH: Am. Soc. Metals Int.) pp 63–76

Kulkarni G J, Banerjee D, Ramachandran T R 1989 Physical metallurgy of aluminium–lithium alloys. *Bull. Mater. Sci.* 12: 325–340

Lagenbeck S L, Sakata I F, Ekvall J C, Reinan R A 1987 Design considerations of new materials for aerospace vehicles. In *Aluminium–lithium alloys: design, development and applications update* (eds) R J Kar, S P Agrawal, W E Quist (Metals Park, OH Am. Soc. Metals Int.) pp 293–314

Lavernia E J, Srivatsan T S, Mohammed F A 1990 Review – strength, deformation, fracture behaviour and ductility of aluminium–lithium alloys. *J. Mater. Sci.* 25: 1137–1158

Lewandowski J J, Holroyd N J H 1990 Intergranular fracture of Al–Li alloys: Effects of aging and impurities. *Mater. Sci. Eng.* A123: 219–227

Lewis R D, Webster D, Palmer I G 1978 Technical Report AFML-TR-78, DARPA Order No. 3417, Lockheed Missiles and Space Company, Palo Alto, CA, p. 102

Lin F S, Starke E A 1979 The effect of copper content and degree of recrystallisation on the fatigue resistance of 7XXX type aluminium alloys: I. Low cycle corrosion fatigue. *Mater. Sci. Eng.* 39: 27–41

Lin F S, Chakravorty S B, Starke E A 1982 Microstructure-property relationships of two Al-3Li–2Cu–0·2XCd alloys. *Metall. Trans.* A13: 401–410

Lynch S P 1991 Fracture of 8090 Al–Li plate–I. Short transverse fracture toughness. *Mater. Sci. Eng.* A136: 25–43

Madhusudhan Reddy G 1998 *Studies on the application of pulsed current and arc oscillation techniques on aluminium–lithium alloy welds*. Doctoral thesis, Indian Institute of Technology, Chennai

Madhusudhan Reddy G, Gokhale A A 1993 Gas tungsten arc welding of AA 8090 Al–Li alloy. *Trans. Indian Inst. Metals* 46: 21–31

Madhusudhan Reddy G, Gokhale A A, Prasada Rao K 1998a Effect of filler metal composition on the weldability of Al–Li alloy welds. *Sci. Technol. Welding Joining* 3: 151–158

Madhusudhan Reddy G, Gokhale A A, Prasada Rao K 1998b Optimisation of pulse frequency in pulsed current gas tungsten arc welding of aluminium–lithium alloy weld. *Mater. Sci. Technol.* 14: 61–68

Masumoto T, Inoue A 1998 Bulk amorphous and nanocrystalline Al-based alloys with high strength. In *Aluminium alloys: Their physical and mechanical properties* (Tokyo: Japan Inst. of Light Metals)

McDarmaid D S, Peel C J 1989 Aspects of damage tolerance in 8090 sheet. In *Aluminium–lithium alloys* (eds) T H Sanders, E A Starke (Birmingham: Mater. Components Eng. Publ.) vol. 2, pp 993–1002

McEvily A J, Ritchie R O 1998 Crack closure and the fatigue crack propagation threshold as a function of load ratio. *Fatigue Fracture Eng. Mater. Struct.* 21: 847–855

McMaster F J, Tabrett C P, Smith D J 1998 Fatigue crack growth rates in Al–Li alloy 2090: Influence of orientation, sheet thickness and specimen geometry. *Fatigue Fracture Eng. Mater. Struct.* 21: 139–150

Meng L, Zheng X L, Tu J P, Liu M S 1998 Effects of deleterious impurities and cerium modification on intrinsic and extrinsic toughening levels of Al–Li based alloys. *Mater. Sci. Technol.* 14: 585–591

Meng L, Tian L, Zheng X L 2000 Notch strength and stress concentration sensitivity of alloy 2090 with various cerium contents. *J. Mater. Sci.* 35: 1481–1486

Meyer P, Cans Y, Ferton D, Reboul M 1987 The metallurgy of industrial Al–Li alloys. *J. Phys. (Paris)* 48: c3.131–c3.138

Miller W S, White J, Reynolds M A, McDermaid D S, Starr G M 1987 Aluminium–lithium–copper–magnesium–zirconium alloys with high strength and high damage tolerance–solving the perceived dichotomy, *J. Phys. (Paris)* 48: c3.131–c3.138

Miura Y, Yusu K, Aibe S, Furukawa M, Nemoto M 1989 Formation and stability of orowan loops in Al–Li single crystals. In *Aluminium–lithium alloys* (eds) T H Sanders, E A Starke (Birmingham: Mater. Components Eng. Publ.) pp 827–836

Mukhopadhyay A K 1988 Doctoral thesis, University of London, London

Mukhopadhyay A K, Flower H M, Steppard T 1990a Development of microstructure in AA 8090 alloy produced by extrusion processing. *Mater. Sci. Technol.* 6: 461–468

Mukhopadhyay A K, Flower H M, Steppard T 1990b Development of mechanical properties in AA 8090 alloy produced by extrusion processing. *Mater. Sci. Technol.* 6: 611–620

Noble B, Harris S J, Dinsdale K 1982 Yield characteristics of aluminium–lithium alloys. *Metall. Sci.* 16: 425–430

Oh Y J, Lee B S, Kwon S C, Hong J H, Nam S W 1999 Low cycle fatigue crack initiation and break in strain-life curve of Al–Li 8090 alloy. *Metall. Mater. Trans.* A30: 887–890

Palmer I G, Miller W S, Lloyd D J, Bull M J 1986 Plastic deformation of Al–Li single crystals. In *Aluminium–lithium alloys* (eds) C Baker, P J Gregson, S J Harris, C J Peel (London: Inst. Metals) vol. 3, pp 565–575

Peel C J 1989 The development of aluminium–lithium alloys: An overview. In *New light alloys* (Neuilly-sur-Seine, France: AGARD)

Peel C J, Evans B, Baker C A, Bennet D A, Gregson P J, Flower H M 1984 The development and application of improved aluminium–lithium alloys. In *Aluminium–lithium alloys* (eds) T H Sander, E A Starke (Warrendale, PA: Metall. Soc. AIME) vol. 2, pp 363–392

Peel C J, McDarmaid D, Evans B 1988 Considerations of critical factors for the design of aerospace structures using current and future aluminium–lithium alloys. In *Aluminium–lithium alloys – design,*

development and applications update (eds) R J Kar, S P Agrawal, W E Quist (Metals Park, Ohio: ASM Int.) pp 315–337

Peters M, Lutjering G 1976 Influence of grain size on tensile properties of a Ti-Mo alloy with precipitate free zones. *Z. Metallk.* 67: 811–814

Petit J, Suresh S, Vasudevan A K, Malcolm R C 1986 Constant amplitude and post-overload fatigue crack growth in Al–Li alloys. In *Aluminium–lithium alloys* (eds) C. Baker, P J Gregson, S J Harris, C J Peel (London: Inst. Metals) vol. 3, pp 257–262

Pickens J R, Heubaum F H, Langan T J, Kramer L S 1989 Al–(4·5–6·3) Cu–1·3 Li–0·4 Ag–0·4 Mg–0·14 Zr alloy weldalite 049. In *Aluminium–lithium alloys* (eds) T H Sanders, E A Starke (Birmingham: Mater. Comp. Eng. Publ.) vol. 3, pp 1397–1411

Pickens J R 1990 Review: recent developments in the weldability of lithium-containing aluminium alloys. *J. Mater. Sci.* 25: 3035–3047

Polmear I J 1995 In *Light alloys* 3rd edn (Arnold Publications) p. 101

Quist W E, Narayanan G H 1989 Aluminium–lithium alloys. In *Aluminium alloys – Contemporary research and applications treatise on materials science and technology* (eds) A K Vasudevan, R D Doherty (San Diego, CA: Academic Press) pp 219–254

Rading G O, Berry J T 1996 On deviated and branched crack paths in Al–Li–X alloys. *Mater. Sci. Eng.* A219: 192–201.

Radmilovic V, Fox A G, Fisher R M, Thomas G 1989 Lithium depletion in precipitate free zones (PFZ's) in Al–Li base alloys. *Scr. Metall.* 23: 75–79

Reynolds M A, Creed E 1987 The development of 8090 and 8091 alloy extrusions. *J. Phys. (Paris)* 48: c3.195–c3.207

Reynolds M A, Gray A, Creed E, Jordan R M, Titchener A P 1986 Processing and properties of alcan medium and high strength Al–Li–Cu–Mg alloys in various product forms. In *Aluminium–lithium alloys* (eds) C. Backer, P J Gregson, S J Harris, C J Peel (London: Inst. Metals) vol. 3, pp 57–65

Sanders T H, Starke E A 1976 The relationship of microstructure to monotonic and cyclic straining of two age hardening aluminium alloys. *Metall. Trans.* A7: 1407–1418

Sanders T H, Starke E A 1982 The effect of slip distribution on the monotonic and cyclic ductility of Al–Li binary alloys. *Acta Metall.* 30: 927–939

Sanders T H, Starke E A 1989 The physical metallurgy of aluminium–lithium alloys - A review. In *Aluminium–lithium alloys* (eds) T H Sanders, E A Starke (Birmingham: Mater. and Component Eng. Publ.) vol. 1, pp 1–37

Sanders T H, Ludwiczak E A, Sawtell R R 1980 The fracture behaviour of recrystalized Al–2·8%Li–0·3%Mn sheet. *Mater. Sci. Eng.* 43: 247–260

Sankaran K K, Grant N J 1980 The structure and properties of splat-quenched aluminium alloy 2024 containing lithium additions. *Mater. Sci. Eng.* 44: 213–227

Sankaran K K, O'Neal J E 1984 Structure-property relationships in Al–Cu–Li alloys. In *Aluminium–lithium alloys* (eds) T H Sanders, E A Starke (Warrendale, PA: Metall. Soc. AIME): vol. 2, pp 393–405.

Satya Prasad K 1999 *Solid state phase transformations in aa 8090 Al–Li alloys*. Doctoral thesis, University of Roorkee, Roorkee

Satya Prasad K, Mukhopadhyay A K, Gokhale A A, Banerjee D, Goel D B 1994 δ precipitation in an Al–Li–Cu–Mg–Zr alloy. *Scr. Metall. Mater.* 30: 1299–1304

Satya Prasad K, Gokhale A A, Mukhopadyay A K, Banerjee D, Goel D B 1999 On the formation of facetted Al3Zr (β') precipitates in Al–Li–Cu–Mg–Zr alloys. *Acta Mater.* 47: 2581–2592

Satya Prasad K, Gokhale A A, Mukhopadhyay A K, Banerjee D, Goel D B 2000 Sequence of precipitation of T_2 and δ phases during aging of Al–Li alloy 8090C. *Mater. Sci. Forum* 331–337: 1043–1048

Satya Prasad K, Vijaya Singh, Gokhale A A 2001 Microstructure of homogenised Al–Sc–Zr alloys. (unpublished work)

Shin K S, Kim S S, Lee E W 1989 Hydrogen embrittlement of a 2090 Al–Li alloy. In *Aluminium–lithium alloys* (eds) T H Sanders, E A Starke (Birmingham: Mater. Components Eng. Publ.) vol. 3, pp 1319–1328

Singh V, Sundararaman M, Chen W, Wahi R P 1991 Low-cycle fatigue behaviour of nimonic PE16 at room temperature. *Metall. Trans.* A22: 499–506

Singh A K, Saha G G, Gokhale A A, Ray R K 1998 Evolution of texture and microstructure in a thermomechanically processed Al–Li–Cu–Mg alloy. *Metall. Mater. Trans.* A29: 665–675

Singh A K, Gokhale A A, Saha G G, Ray R K 1999 Texture evolution and anisotropy in Al–Li–Cu–Mg alloys. In *Textures in materials research* (eds) R K Ray, A K Singh (New Delhi: Oxford and IBH) pp 219–234

Singh A K, Gokhale A A, Satya Prasad K 2001 (Unpublished work)

Srivatsan T S, Coyne E J 1986 Cyclic stress response and deformation behaviour of precipitation - hardened aluminium–lithium alloys. *Int. J. Fatigue* 8: 201–208

Srivatsan T S, Coyne E J 1987 Mechanisms governing cyclic fracture in an Al–Cu–Li alloy. *Mater. Sci. Technol.* 3: 130–138

Srivatsan T S, Yamaguchi K, Starke E A 1986 The effects of environment and temperature on the low cycle fatigue behaviour of aluminium–alloy 2020. *Mater. Sci. Eng.* 83: 87–107

Srivatsan T S, Hoff T, Prakash A 1991 The high strain cyclic fatigue and fracture behaviour of 2090 aluminium alloy. *Eng. Fracture Mech.* 40: 297–309

Starke E A, Lin F S 1982 The influence of grain structure on the ductility of the Al–Cu–Li–Mn–Cd alloy 2020 *Metall. Trans.* A13: 2259–2269

Starke E A, Quist W E 1989 The microstructure and properties of aluminium–lithium alloys. In *New light alloys* (Neuilly-sur-Seine, France: AGARD) pp 4·1–4·23

Starke E A, Sanders T H, Palmer I G, 1981 New approaches to alloy development in the Al–Li system. *J. Metals* 33: 24–32

Sundararaman M, Chen W, Singh V, Wahi R P 1990 TEM investigation of γ' free bands in nimonic PE16 under LCF loading at room temperature. *Acta Metall. Mater.* 38: 1813–1822

Sunder R 1991 Engineering analysis of notch root fatigue crack growth under spectrum loading. *Int. J. Fatigue* 13: 249–262

Suresh S, Ritchie R O 1984 Propagation of short fatigue cracks. *Int. Metals Rev.* 29: 445–476

Suresh S, Vasudevan A K, Bretz P E 1984 Mechanisms of slow fatigue crack growth in high strength aluminium alloys: Role of microstructure and environment. *Metall. Trans.* A15: 369–379

Suresh S, Vasudevan A K, Tosten M, Howell P R 1987 Microscopic and macroscopic aspects of fracture in lithium containing aluminium alloys. *Acta Metall.* 35: 25–46

Sverdlin A, Drits A M, Krimova T V, Sergeev K N, Ginko I B 1998 Aluminium–lithium alloys for aerospace. *Adv. Mater. Process.* 6: 49–51

Tintillier R, Gudladt H J, Gerold V, Petit J 1989 Near threshold fatigue crack growth in high purity binary Al–Li single crystals. In *Aluminium–lithium alloys* (eds) T H Sanders, E A Starke (Birmingham: Mater. Components Eng. Publ.) vol. 2, pp 1135–1146

Toropova L S, Eskin D G, Kharakterova M L, Dobtkina T V 1998 *Advanced aluminium alloys containing scandium* (The Netherlands: Gordon and Breach Science Publ.) pp 133–167

Vasudevan A K, Doherty R D 1987 Grain boundary ductile fracture in precipitationhardened aluminium alloys. *Acta Metall.* 35: 1193–1219

Vasudevan A K, Suresh S 1985 Lithium-containing aluminium alloys. Cyclic fracture. *Metall. Trans.* A16: 475–477

Vasudevan A K, Bretz P E, Miller A C, Suresh S 1984 Fatigue crack growth behavior of aluminium alloy 2020 (Al–Cu–Li–Mn–Cd). *Mater. Sci. Eng.* 64: 113–122

Vasudevan A K, Ludwiczak E K, Baumann S F, Howell P R, Doherty R D, Kersker M M 1986 Grain boundary fracture in Al–Li alloys. *Mater. Sci. Technol.* 2: 1205–1209

Vasudevan A K, Doherty R D, Suresh S 1989 Fracture and fatigue characteristics in aluminium alloys. In *Aluminium alloys - Contemporary research and applications. Treatise on materials science and technology* (eds) A K Vasudevan, R D Doherty (San Diego, CA: Academic Press) pp 445–462

Venkateswara Rao K T, Ritchie R O 1989a Mechanical properties of aluminium–lithium alloys: Part – I. Fracture toughness and microstructure. *Mater. Sci. Technol.* 5: 882–895

Venkateswara Rao K T, Ritchie R O 1989b Mechanical properties of aluminium–lithium alloys: Part – II. Fatigue crack propagation. *Mater. Sci. Technol.* 5: 896–905

Venkateswara Rao K T, Ritchie R O 1990 Mechanisms influencing the cryogenic fracture-toughness behaviour of aluminium–lithium alloys. *Acta Metall.* 38: 2309–2326

Venkateswara Rao K T, Ritchie R O 1992 Fatigue in aluminium–lithium alloys. *Int. Mater. Rev.* 37: 153–185

Venkateswara Rao K T, Yu W, Ritchie R O 1988a Fatigue crack propagation in aluminium–lithium alloy 2090: Part I. Long crack behaviour. *Metall. Trans.* A19: 549–561

Venkateswara Rao K T, Yu W, Ritchie R O 1988b Fatigue crack propagation in aluminium–lithium alloy 2090: Part II. Small crack behaviour. *Metall. Trans.* A19: 563–569

Venkateswara Rao K T, Bucci R J, Jata K V, Ritchie R O 1991 A comparison of fatigue-crack propagation behaviour in sheet and plate aluminium–lithium alloys. *Mater. Sci. Eng.* A141: 39–48

Vijaya Singh 1997 *Preparation and characterisation of Al–Li–Cu–Mg–Zr based alloys*. Doctoral thesis, Banaras Hindu University, Varanasi

Vijaya Singh, Chakravorty C R 1989 Melting and casting of Al–Li alloys – A review. In *Science and technology of aluminium–lithium alloys* (Bangalore: Hindusthan Aeronautics) pp 83–91

Vijaya Singh, Gokhale A A 2000 Control of grain structure through transition element additions in an Al–Li base alloy. *Mater. Sci. Forum* 331–337: 477–482

Vijaya Singh, Satya Prasad K, Gokhale A A 2001 Effect of Zr and Sc additions on the as-cast structure of aluminium. *Int. J. Cast Metals Res.* (submitted)

Wadsworth J, Palmer I G, Crookes D D, Lewis R E 1984 Superplastic behaviour of aluminium–lithium alloys, in *Aluminium–lithium alloys* (eds) T H Sanders, E A Starke (Warrendale, PA: Metall. Soc. AIME) pp 111–135

Wadsworth J, Heusahall C A, Nieh T E 1986 Superplastic aluminium–lithium alloys. In *Aluminium–lithium alloys* (eds) C Backer, P J Gregson, S J Harris, C J Peel (London: Inst. Metals) pp 199–212

Wanhill R J H 1994 Status and prospects for aluminium–lithium alloys in aircraft structures. *Int. J. Fatigue* 16: 3–20

Wanhill R J H, Hart W G J-t', Schra L 1991 Flight simulation and constant amplitudefatigue crack growth in aluminium–lithium sheet and plate. In *Aeronautical fatigue: Key to safety and structural integrity* (Warley, UK: Engineering Materials Advisory Series) pp 393–430

Warren C J, Rioja R J 1989 Forming characteristics and post-formed properties of Al–Li alloys. In *Aluminium–lithium alloys* (eds) T H Sanders, E A Starke (Birmingham: MCEP) pp 417–429

Webster D 1987 The effect of low melting point impurities on the properties of aluminium–lithium alloys. *Metall. Trans.* A18: 2187–2193

Welpmann K, Peters M, Sanders T H 1984 Aluminium–lithium alloys. *Aluminium* 60: E641–E646

Wert J A, Lumsden J B 1985 Intergranular fracture in an Al–Li–Cu–Mg–Zr alloy. *Scr. Metall.* 19: 205–209

Westwood A R C 1990 New materials for aerospace industry. *Mater. Sci. Technol.* 6: 958–961

Williams D B, Howell P R 1989 The microstructure of aluminium–lithium based alloys. In *Aluminium alloys - Contemporary research and applications. Treatise on materials science and technology* (eds) A K Vasudevan, R D Doherty (San Diego, CA: Academic Press) pp 219–254